Available online at www.sciencedirect.com
SCIENCE DIRECT®
Precambrian Research 134 (2004) 143–167
Precambrian Research
www.elsevier.com/locate/precamres

Whole-rock and Nd isotopic geochemistry of Neoarchaean granitoids and their bearing on the evolution of the Central Hearne supracrustal belt, Western Churchill Province, Canada

H.A. Sandeman*[,1], S. Hanmer, W.J. Davis, J.J. Ryan[2], T.D. Peterson

Geological Survey of Canada, 601 Booth St., Ottawa, Ont., Canada K1A 0E8

Received 19 June 2003; accepted 6 May 2004

Abstract

The Central Hearne supracrustal belt (CHSB), Hearne domain, Western Churchill Province forms a large (ca. 30,000 km^2), greenschist grade Neoarchaean (2711–2660 Ma) terrane of predominant metavolcanic and less common metasedimentary rocks intruded by three groups of plutonic rocks. Pre-tectonic group 1 plutons (>2690 Ma) include rare gabbro, dominant diorite to tonalite and rare granodiorite and granite. These intrude and incorporate angular inclusions of cogenetic volcanic rocks and have variably developed foliations. Syn-tectonic group 2 plutons (2690–2679 Ma) comprise rare gabbro and diorite, predominant tonalite and granodiorite and rare granite, and exhibit N–S-trending, ductiley deformed supracrustal schlieren-rich intrusive margins. Post-tectonic group 3 plutons are rare, and comprise either potassic, biotite monzogranite or alkalic nepheline syenite and rare carbonatite. Abundant tonalite to granodiorite, biotite ± hornblende – bearing mineralogies and metaluminous and generally low-medium K_2O compositions, indicate that most rocks are I- or M-type granitoids. Molecular Na–Ca–K variations and AFM indices indicate transitional calc-alkaline – trondjhemitic trends with both tholeitic and calc-alkaline affinities. Rare earth and incompatible element variations suggest that most granitoids exhibit volcanic arc- or tonalite–trondhjemite–granodiorite (TTG)-like abundances with multi-element patterns varying gradationally from La-poor ($La_N/Yb_N < 12$) to La-rich compositions ($La_N/Yb_N > 12$). Nd isotopic values overlap with contemporaneous depleted mantle indicating that the granitoids represent melts derived from predominantly juvenile mantle or crust. La-poor rocks likely formed through low-*P* anatexis of amphibolitic crust with plagioclase + amphibole ± clinopyroxene present, whereas high-La rocks were generated via high-*P* partial melting of a garnet + clinopyroxene-bearing protolith (plausibly a subducted slab). Granitoid evolution from early dominant low-*P*, tholeiitic and calc-alkaline melts, to later, predominant high-*P*, high-Al_2O_3 TTG melts, reflects a change in the tectonomagmatic setting at ca. 2690 Ma. Construction of proto-arc crust from ca. 2711–2690 Ma, and extension of the leading edge of normal (ca. 40 km) Archaean oceanic crust, in response to lithospheric processes analogous to those of the Eocene SW Pacific Ocean, resulted in asthenospheric upwelling, intrusion of mantle-derived melts into the lower crust, and their subsequent ascent and fractionation. Partial melting at the base of the extended, thick oceanic crust likely yielded sparse high-La melts at this time. At ca. 2690 Ma, a change from an extensional to a shortening regime resulted in initiation of subduction of adjacent oceanic lithosphere, partial melting of the eclogitic downgoing slab and generation of voluminous, high-*P*, La-rich granitoid magmas. This yielded less

*Corresponding author.
E-mail address: hsandema@nrcan.gc.ca (H.A. Sandeman).
[1]Current address: Canada-Nunavut Geoscience Office, 626 Tumiit Building, P.O. Box 2319, Iqaluit, Nunavut X0A 0H0.
[2]Current address: Geological Survey of Canada, Pacific Division, Vancouver Office, 101-605 Robson Street, Vancouver, BC, Canada V6B 5J3.

0301-9268/$ – see front matter.
doi:10.1016/j.precamres.2004.05.005

abundant low-*P*, La-poor melts emplaced into the "infant-arc" crust during and following tectonism. The complete sequence was intruded by late potassic granites derived from tonalitic lower crust and alkalic magmas that originated in the lithospheric mantle.

Keywords: Neoarchaean; Western Churchill Province; Central Hearne domain; Granitoids; Petrogenesis; Volcanic arc; TTG suites

1. Introduction

Much of our present understanding of early Earth's evolution and the role or indeed existence of Archaean tectonics has arisen from the systematic investigation of Precambrian greenstone belts. Historically, many of the salient observations, including lithological, structural, geochronological and petrochemical data, have been obtained from supracrustal sequences and, in particular, their contained volcanic rocks (e.g., Thurston and Chivers, 1990 and references therein; de Wit and Ashwal, 1997 and references therein; Tomlinson and Condie, 2001; Mueller et al., 2002 and references therein). Although much recent work has focused on the distribution, petrogenesis and the role of plutonism in Archaean crustal development (e.g., Chown et al., 2002; Martin and Moyen, 2002; Whalen et al., 2002; Bédard et al., 2003; Smithies et al., 2004), these studies of intrusive rocks are significantly less common than those of their volcanic counterparts, even though Archaean rocks exposed at surface are commonly dominated by plutonic assemblages. Moreover, investigations that directly integrate the temporal and petrogenetic evolution of the collective volcanic supracrustal and plutonic infracrustal components of greenstone belts have rarely been presented.

Recent work (e.g., Defant and Drummond, 1990; Drummond and Defant, 1990; Drummond et al., 1996), focused on the geochemical characteristics of arc-related, high-MgO andesites (adakites), has suggested that Archaean tonalite–trondhjemite–granodiorite suites (TTG or TTD; Arth and Barker, 1976; Martin, 1986, 1995) have similar petrogeneses. Moreover, the compositions of these rocks are compatible with the experimental work of Sen and Dunn (1994) and Rapp et al. (1999), under such simulated conditions. This concept has become widely accepted as the predominant mechanism responsible for the generation of TTG magmas (Martin, 1986, 1995, 1999; Whalen et al., 1999). This hypothesis suggests that high-Mg andesites (adakites) and Archaean TTG suites can be produced through partial melting of mafic crust at high-*P* (transformed to eglogite; 1–4 GPa) coupled with subsequent interaction of the magmas with overlying peridotitic asthenosphere (Sen and Dunn, 1994; Martin, 1999; Rapp et al., 1999). On the basis of major element and experimental data, however, Smithies (2000) and Petford and Gallagher (2001) questioned this idea and proposed an alternative process involving anatexis of hydrous, mafic lower crust. Similarly, Kamber et al. (2002) determined on the basis of trace element constraints that TTG magmas strongly resemble ordinary, mantle wedge-derived arc magmas, that they do not form via slab melting and likely form from extensive fractional crystallization of mafic precursors. If these authors are correct, then upwelling of fluid modified mantle beneath thickened oceanic lithosphere may be all that is required to generate Archaean TTG magmatic suites.

In this contribution, we present field, lithogeochemical and Nd isotopic data for plutonic rocks from the Kaminak segment of the Central Hearne supracrustal belt (CHSB), western Churchill Province Canada, supplementing and enhancing the observations and conclusions presented in our companion papers (Cousens et al., in press; Davis et al., in press; Hanmer et al., in press; Sandeman et al., 2004). We divide the granitoids of the CHSB into three major temporal groups (1–3; note that the geographical distribution of granitoids into groups 1 through 3 is given in Fig. 2 of Davis et al., 2004). In particular, we focus on the voluminous group 2 tonalite–granodiorite plutons that are broadly contemporaneous with the emplacement of the intermediate to felsic sequences of volcanic assemblage II as outlined by Hanmer et al. (in press), Davis et al. (2004) and Sandeman et al. (2004). As will be shown here, supporting Nd isotopic data suggests derivation of all of the plutonic rocks from variably

depleted, predominantly juvenile Neoarchaean mantle or crust. Whole-rock lithogeochemistry demonstrates that the majority of the group 1 and some of the group 2 granitoids were formed through mantle input into the lower crust, low- to moderate-*P* partial melting of the basaltic lower crust in the presence of plagioclase + amphibole ± garnet with subsequent fractionation of quartz–feldspar ± biotite ± amphibole mineral assemblages in mid- to upper-crustal magma chambers. In contrast, a large proportion of the group 2 and many of the group 3 rocks exhibit lithogeochemical features indicating that they were derived via higher-*P* partial melting of a clinopyroxene + garnet protolith and that many of the derived magmas may have interacted with asthenospheric peridotite during ascent.

2. Geologic setting

The western Churchill Province can be divided into Rae and Hearne domains, separated by the Snowbird Tectonic zone (Fig. 1; Hoffman, 1988). In the Hearne domain, supracrustal belts collectively termed the Rankin–Ennadai greenstone belt (Wright, 1967) comprise a number of discrete, geologically distinct supracrustal belts. Extensive field, geochronological, metamorphic, petrochemical and Nd isotopic data permit the subdivision of the Hearne domain into central and northwestern subdomains (Hanmer and Relf, 2000), the former of which has historically been studied in three contiguous areas comprising, from SW to NE, the Henik, Kaminak and Tavani segments (see Hanmer et al., in press).

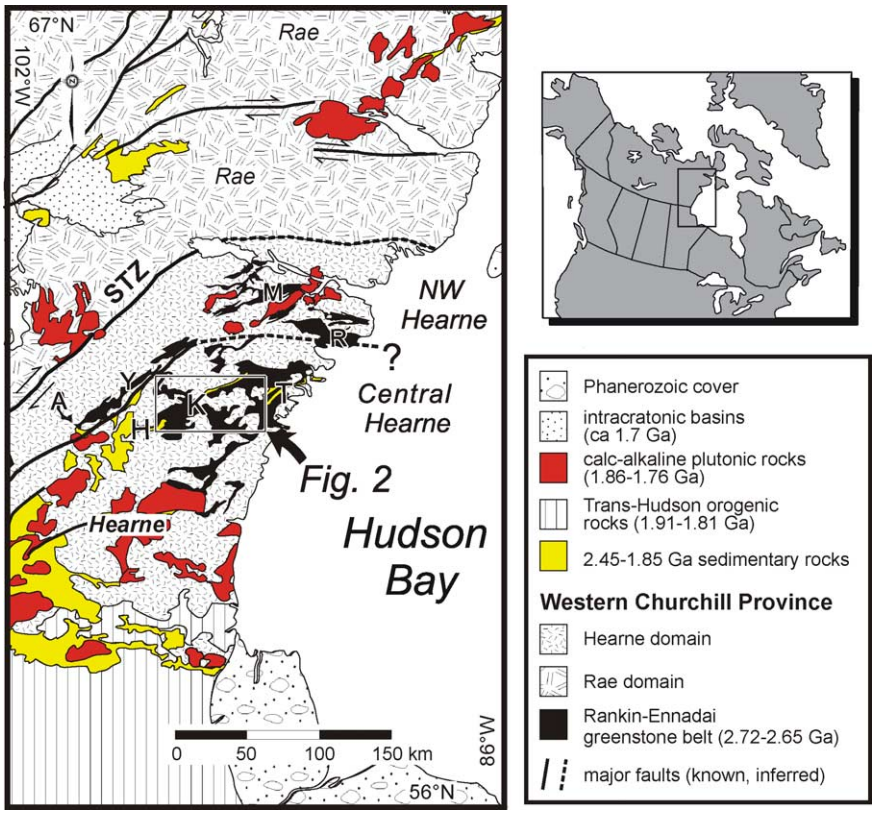

Fig. 1. Simplified geological map of the Western Churchill Province in the northcentral Canadian Shield showing the location of the study area (inset) with respect to the major lithotectonic domains of the region. Shown are the approximate boundaries between the northwestern and central Hearne subdomains (Hanmer and Relf, 2000), and the locations of the different segments of the Rankin-Ennadai greenstone belt. Key: Kaminak segment = K; Tavani segment = T; Henik segment = H; Rankin segment = R; MacQuoid segment = M; Yathkyed segment = Y; Angikuni segment = A; and STZ = Snowbird Tectonic zone (Hoffman, 1988).

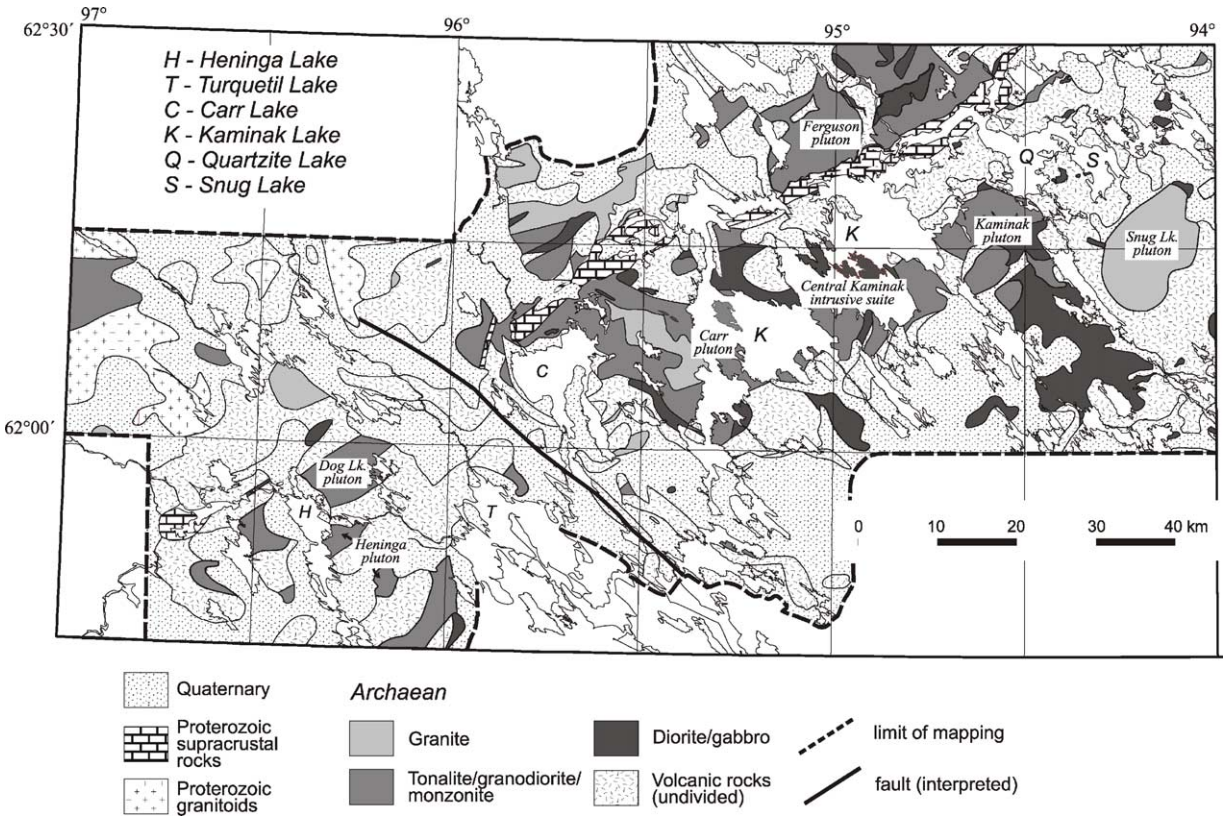

Fig. 2. Simplified geological map of the CHSB from Heninga to Quartzite Lake. The locations of the major plutons discussed in the text are shown (Table 1). The geographic distribution of granitoids of groups 1 through 3 are given in Fig. 2 of Davis et al. (in press).

The Central Hearne supracrustal belt (Figs. 1 and 2) is a composite volcanic–plutonic package characterised by well-preserved, typically greenschist-facies volcanic and sedimentary units ranging in age from 2711 to 2681 Ma (Cousens et al., in press; Davis et al., in press; Hanmer et al., in press). The volcanic rocks of the Henik–Kaminak–Tavani corridor can be divided into two distinct tectono-magmatic assemblages that are collectively referred to as the Kaminak group in the Kaminak segment (Davis et al., in press; Hanmer et al., in press; Sandeman et al., 2004). Assemblage I (2711–2691 Ma) comprises predominantly pillowed and massive mafic to intermediate volcanic and volcaniclastic rocks with subordinate, intercalated intermediate to felsic flows and tuffs. Assemblage II (2686–2681 Ma) comprises less abundant mafic volcanic rocks that are closely associated with voluminous intermediate volcaniclastic debris flows, tuffs and subordinate rhyolitic lavas and their subvolcanic equivalents. Volcanic assemblage I was intruded initially at ca. 2691 Ma by gabbro, diorite and rae tonalite to granite intrusions. Assemblages I and II were then intruded at ca. 2686–2679 Ma (Davis et al., in press) by voluminous and compositionally varied intermediate (tonalite–granodiorite) plutons that dominate the overall geological map pattern (Fig. 2). All of the above units were subsequently intruded by group 3 plutons that range in age from ca. 2666–2659 Ma (Cavell et al., 1992; Davis et al., in press).

3. Field relationships and petrography

We define three major groups of plutonic rocks exposed in the Kaminak segment of the CHSB. *Group 1* plutons are syn- to late-volcanic with respect to

volcanic assemblage I and predate the first phase of deformation. *Group 2* plutons are considered to have been emplaced contemporaneously with the late stages of assemblage II volcanism and synchronous with a second major regional deformation event. *Group 3* plutons represent late, post-tectonic intrusions. Group 1 and group 2 plutons are deformed, whereas those of group 3 are undeformed. Nine spatially discrete plutons are presently defined; their petrological characteristics and U–Pb ages are outlined in Table 1 and their locations are given in Fig. 2. All ages discussed are ID thermal ionization mass spectrometry determinations on zircon (with 2σ error) unless otherwise indicated.

3.1. Group 1 (syn-volcanic assemblage I units)

The oldest plutonic rocks in the belt constitute the Central Kaminak intrusive suite (CKIS), a number of discontinuous, areally extensive (ca. 500 km^2), irregularly shaped composite plutons that dominate the central and southeastern parts of the Kaminak segment of the belt, respectively (Fig. 2). These appear to have experienced one and locally two phases of deformation (Hanmer et al., 1998, in press). The CKIS comprises abundant diorite with subordinate tonalite and granite that intrude volcanic rocks of assemblage I.

The CKIS is characterized by at least three texturally distinct dioritic units that exhibit complex, commonly mutual cross-cutting relationships, and include macroscopic evidence of magmatic commingling. These units include: (1) a medium- to fine-grained, equigranular hornblende + biotite + titanite leucodiorite dated at 2691 ± 1 Ma (Table 1; Davis et al., 2000) (in press); (2) plagioclase porphyritic to megacrystic hornblende diorite; and (3) hornblende oikocrystic (<3 cm) diorite. Many outcrops comprise mixtures of these three. The diorites intrude and locally grade into adjacent hypabyssal and extrusive units of the Kaminak group (Hanmer et al., in press) and commonly contain abundant cm- to

Table 1
Subdivision of the plutonic rocks of the CHSB according to petrological group, age and selected petrochemical characteristics

Pluton name	Mineralogy and description	Age[a] (Ma)	Ranges in critical petrochemical indices			ΣREE
			Mg#	La_N/Yb_N	Eu/Eu*	
Group 1 units						
Central Kaminak	GB to Hb-Ttn DR	2691 ± 1	0.20–0.76	1.0–7.5	0.83–1.99	17–133
intrusive complex	Bt TN		0.49–0.56	9.4–22.7	0.77–1.14	80–254
	Bt MG		0.19–0.37	5.2–41.7	0.39–0.81	128–202
Group 2 units						
Carr pluton	Hb-Ttn DR	0.50–0.62	18.7	0.88	197	
	Bt TN to Bt GD	2686^{+2}_{-1}	0.21–0.68	4.8–62.3	0.60–1.11	38–320
	Bt MG		0.26–0.92	1.1–89.7	0.07–2.16	29–515
	Hb-Bt MZ	2682 ± 2	0.30–0.50	88.1–156.9	0.70–1.06	778–1299
Kaminak pluton	Rare GB to Hb DR		0.39–0.57	2.2–5.1	0.88–1.64	34–73
	Hb-Bt TN to GD	2679^{+3}_{-2}	0.48–0.55	6.8–22.44	0.72–0.94	101–131
Ferguson pluton	Rare GB to Hb DR		na	na	na	na
	Hb-Bt TN to GD	ca. 2680	0.54–0.66	3.7–49.8	0.80–0.95	93–229
Heninga pluton	Hb-Bt TN to GD	ca. 2680	0.34–0.43	7.8–12.1	0.55–0.99	71–164
Dog Lake Pluton	Bt GD to MG	ca. 2680	0.46–0.57	31.4–49.9	0.74–1.16	64–86
Group 3 units						
Snug Lake pluton	Ksp phy Bt MG	2666 ± 1	0.33–0.35	67.6–74.3	0.74–0.82	268–395
Kaminak Lake	Np SYEN, IJOL, JAC	2659 ± 5[b]	0.27–0.77	27.3–109.2	0.84–0.97	435–1392
Alkaline complex	Rare CB		na	na	na	na

Key: GB = gabbro; DR = diorite; TN = tonalite; GD = granodiorite; MG = monzogranite; MZ = monzonite; SYEN = syenite; JAC = jacupirangite; CB = carbonitite; phy = phyric; Hb = hornblende; Bt = biotite; Ksp = potassium feldspar; Ttn = titanite; Np = nepheline; a = U–Pb, IDTIMS zircon age; b = U–Pb, SHRIMP zircon age (Cavell et al., 1992); na = not available; Mg# = molecular MgO/FeO^T + MgO; La_N/Yb_N = chondrite normalized (Sun and McDonough, 1989); Eu/Eu*, after Taylor and McLennan (1985). All ages except for the Kaminak Lake alkaline complex (Cavell et al., 1992) are from Davis et al. (in press). Those in parentheses are inferred, based on field, petrological and geochemical features.

metre-scale xenoliths of locally derived supracrustal rocks. Tonalites of the CKIS are less abundant, and occur only along the eastern and southern margin of the complex where they typically comprise metre- to 100 metre-scale sheets that intrude the diorites. The tonalites are biotite-bearing and contain abundant supracrustal screens and rafts of metavolcanic rocks. Granitic rocks are rare and comprise biotite-bearing, equigranular monzogranite veins and sheets that intrude all other phases.

3.2. Group 2 (syn-postvolcanic assemblage II units)

The most voluminous intrusive rocks in the study area are plutons emplaced synchronously with volcanic assemblage II (2688–2679 Ma; Hanmer et al., in press). This interval is interpreted as heralding a major change in the tectonic environment, reflected by an increase in the volume of felsic to intermediate volcanic rocks, the emplacement of large plutons of intermediate composition and the development of a regional, second generation foliation. These rocks include the Kaminak, Ferguson and Carr plutons (Hanmer et al., 1998; Hanmer et al., in press).

The *Kaminak pluton* (cf. Kaminak Batholith; Davidson, 1970a) ranges from hornblende–biotite–titanite tonalite and granodiorite in the north to rare hornblende gabbro and diorite in the south. Hornblende grains range up to 10 mm in diameter, lending all rocks a porphyritic appearance. Microcline is typically paragenetically late and forms uncommon, large ($\leq$8 mm) oikocrysts surrounding most other phases. The pluton is mantled on its northern margin by intrusive breccias incorporating rafts and blocks of volcanic rocks of both volcanic assemblages. The western margin of the pluton is defined by hornfelsed, highly strained, banded metavolcanic rocks. Variably deformed veins emanating from the pluton suggest that the country rocks were deformed during, and presumably as a consequence of, pluton emplacement. To the south and east, tonalite and granodiorite of the Kaminak pluton intrude presumably comagmatic (undated) quartz diorite, diorite and rare gabbro. Cavell et al. (1992) obtained a poorly constrained SHRIMP U–Pb zircon age of 2700 $\pm$ 11 Ma for tonalite of the Kaminak batholith, an age refined by Davis et al. (2000) (in press) as 2679^{+3}_{-2} Ma (Table 1).

The *Ferguson pluton*, located north of Kaminak Lake (Fig. 2), is also diverse in composition, ranging from rare gabbro and quartz diorite to abundant tonalite and granodiorite. Tonalite underlies the western part of the pluton, whereas mafic compositions with their volcanic carapace prevail in the east. Quartz diorite and diorite in the east (Fig. 2) contain abundant supracrustal inclusions, and both are intruded by biotite–hornblende tonalite. The pluton is locally extensively altered and primary features are commonly poorly preserved. It generally consists of quartz, plagioclase and variable amounts of microcline surrounded by a chloritic matrix, even where not significantly deformed. Primary magmatic biotite and hornblende are only locally preserved.

The *Carr pluton* varies from diorite to syenogranite and includes at least four distinct plutonic phases. The oldest recognized unit comprises incipiently- to well-foliated, medium- to coarse-grained biotite tonalite with blue quartz phenocrysts that varies gradationally to abundant, homogenous, medium-grained, biotite–hornblende granodiorite. The biotite tonalite is locally associated with a medium-grained hornblende quartz diorite. Diffuse, gradational contacts, the mechanical incorporation of potassium feldspar and quartz grains from the tonalite into the diorite, and hornblende coronae around incorporated quartz grains all suggest commingling of the two magmas. A specimen of the blue quartz tonalite yielded an age of 2686 $\pm$ 2 Ma (Table 1; Davis et al., in press). The tonalite, diorite and granodiorite are collectively cross-cut by veins and dykes of fine- to medium-grained biotite monzogranite that also forms a coherent body in the centre of the pluton (Fig. 2). On the northern and southern margins of the Carr pluton, veins and dykes of granitoid intrude the adjacent country rocks forming a sheeted complex. The northwestern contact is not exposed, but tonalite mapped on the western shore of Carr Lake is likely equivalent to the biotite–hornblende tonalite of the Carr pluton (Fig. 2). The eastern margin of the Carr pluton is defined by a series of margin-parallel, schlieren-rich zones alternating with inclusion-free biotite $\pm$ hornblende tonalite. Over a distance of ca. 4 km, these pass eastwards into the CKIS. To the southwest, medium-grained, homogenous biotite $\pm$ hornblende $\pm$ titanite monzonite intrudes biotite–hornblende granodiorite of the Carr pluton and surrounding volcanic

rocks. This monzonite yielded a crystallization age of 2681 ± 3 (Table 1; Davis et al., in press) and is the youngest phase of the Carr Pluton.

A number of other intermediate intrusions have been mapped in the Kaminak segment, including the large Turquetil pluton (Davidson, 1970a) lying to the south and west of the map area, for which no petrological data are available. Also to the southwest, two small plutons (Fig. 2) intrude a package of diverse, mafic to felsic, volcanic and volcaniclastic rocks, one felsic lithic tuff of which was dated at 2686^{+5}_{-3} Ma (Davis et al., in press). The *Dog Lake pluton* forms a ca. 90 km^2, approximately oval body exposed northeast of Heninga Lake (Fig. 2). The pluton is a massive, variably altered and foliated, granodiorite to tonalite characterized by sparse chloritized biotite set in a saussuritized plagioclase and quartz-rich matrix. Exposed ca. 8 km farther to the south is the *Heninga pluton*, a composite body of variably foliated, fine-grained biotite tonalite intrusions, interpreted as high-level cupolas that intrude felsic and intermediate volcanic rocks of the Kaminak group. Although this unit has not been dated, we interpret it to be ≤2686 Ma in age because it intrudes intermediate volcaniclastic rocks of volcanic assemblage II.

Northwest of Kaminak Lake is a series of generally narrow (≤5 km), foliated, layer-parallel NE-trending granitoid sheets that cross-cut volcanic rocks of the Kaminak group. These are diverse in composition and include fine- to medium-grained biotite tonalite, medium-grained biotite monzogranite, coarse-grained microcline porphyritic biotite monzogranite and minor, fine- to medium-grained gabbro. Because the absolute ages of these granitoids are not known, and their contact relationships are commonly obscured, it is difficult to assign them to groups 1, 2 or 3 suites. It is probable, however, that the monzogranitic, tonalitic and gabbroic rocks correlate with the group 2 plutons, whereas the microcline megacrystic monzogranite resembles the group 3 Snug Lake pluton (see below).

3.3. Group 3 units

The group 3 *Snug Lake pluton* is sporadically exposed in the uplands south of Snug Lake (Fig. 2). This pluton is unfoliated, and comprises coarse-grained, microcline porphyritic (≤3 cm) biotite monzogranite with abundant quartz in the groundmass. Microcline phenocrysts range up to 3 cm in diameter and rare quartz phenocrysts are also locally present. This intrusion cross-cuts both the main structural fabrics in the region and the hornblende isograd, and is thus post-metamorphic and post-tectonic in nature (Relf, 1995; Irwin et al., 1998). It yielded a crystallization age of 2666 ± 1 Ma (Table 1; Davis et al, in press), comparable to late tectonic plutonic rocks of the east Gill Lake pluton of the Tavani segment (2666 ± 2 Ma; Park and Ralser, 1992).

The only other known group 3 unit is the Kaminak Lake alkaline complex (Davidson, 1968, 1970b). This consists of a nested series of silica-undersaturated alkaline intrusive rocks ranging in composition from rare carbonatite through more abundant jacupirangite and ijolite to abundant nepheline syenite. Cavell et al. (1992) presented SHRIMP data on zircons from five compositionally distinct rocks of the alkaline complex, yielding a well-constrained U–Pb concordia age of 2659 ± 5 Ma (2σ). The alkaline rocks are thus younger than all other rocks in the belt (see above), and constitute one of the oldest known alkaline intrusions in the world.

4. Geochemistry

One hundred and seventy-eight whole-rock specimens of intrusive rocks, excluding fine-grained syn-volcanic sills and dykes, were collected throughout the map area (Fig. 2; Table 2). Although the majority of the specimens comprised holocrystalline granitoids, those rocks deemed to be cumulates (i.e., characterised by high MgO with accompanying elevated Ni and Cr, or by strong positive Eu or Sr anomalies on chrondrite normalized or multi-element plots) are excluded from the discussions relating to source components or tectonomagmatic setting.

4.1. Alteration

Alteration of plutonic rocks is a common phenomenon, in particular for Archaean rocks, and is typically characterized by high loss on ignition (LOI) values and increased scatter and mobility of major and large ion lithophile elements (LILE). Some studies have noted, however, that even for rocks of ancient heritage, the concentrations of such “mobile” elements

Table 2
Representative lithogeochemical analyses of rocks from the three temporal plutonic suites of the Kaminak segment of the CHSB

Sample	P610	H32	C250	H522A	H25A	H458A	P124	DMW247	H61A
Group	1	1	1	1	1	1	2	2	2
Pluton	CKIS	CKIS	CKIS	CKIS	CKIS	CKIS	CARR	CARR	CARR
Rock-type	HbDR	HbDR	DR	TN	MG	MG	DR	DR	MZ
wt. %									
SiO_2	51.6	50.5	57.5	67.6	74.0	71.5	50.9	53.1	60.4
TiO_2	0.37	0.76	0.77	0.43	0.25	0.51	0.98	0.82	0.51
Al_2O_3	19.0	16.6	15.5	15.8	12.9	14.1	14.7	15.2	18.4
FeO^T	6.57	9.27	7.47	3.42	2.61	3.33	8.46	8.91	3.91
MnO	0.11	0.17	0.12	0.05	0.02	0.06	0.15	0.15	0.08
MgO	6.03	7.59	4.54	1.81	0.34	0.92	7.74	6.72	2.15
CaO	10.41	9.54	6.89	4.18	1.30	2.90	10.33	9.79	2.83
Na_2O	2.30	2.30	3.50	4.60	4.50	4.30	2.60	2.30	5.06
K_2O	1.18	0.93	2.00	0.86	2.30	1.45	1.27	1.19	3.91
P_2O_5	0.05	0.21	0.28	0.13	0.05	0.11	0.32	0.14	0.27
LOI	2.10	1.50	0.90	0.80	1.60	0.80	1.40	1.40	1.79
Mg#	0.621	0.593	0.520	0.485	0.188	0.330	0.620	0.573	0.495
ppm									
Cr	58	190	130	55	16	20	220	42	bd
Ni	120	200	77	29	bd	bd	130	140	bd
Co	38	48	30	38	33	31	40	39	bd
Sc	22.0	29.0	18.0	7.7	5.6	8.2	30.0	28.0	7.0
V	110	130	140	54	5	31	66	150	56
Cu	14	62	57	bd	bd	68	61	32	6
Pb	18	2	7	20	16	19	5	2	13
Zn	42	85	73	39	26	100	66	81	45
Rb	45	36	72	19	75	27	29	39	64
Ba	230	140	810	360	390	390	420	203	3332
Sr	250	190	410	470	47	190	450	170	777
Nb	2.5	4.9	8.5	4.2	16.0	13.0	8.1	6.4	7.5
Hf	1.5	0.0	4.1	3.2	7.2	6.9	3.1	3.2	3.4
Zr	65	67	190	140	280	270	140	110	473
Y	11	20	25	9	42	32	20	21	18
Th	0.58	0.53	5.70	2.00	7.60	4.70	4.60	2.60	12.53
U	0.17	0.17	1.00	0.21	1.30	1.30	0.69	0.47	1.25
La	5.6	9.1	50.0	17.0	38.0	27.0	39.0	10.0	187.9
Ce	12.0	22.0	110.0	34.0	82.0	60.0	82.0	24.0	363.3
Pr	1.6	2.9	13.0	4.0	9.8	7.1	11.0	3.2	41.3
Nd	6.4	14.0	54.0	15.0	37.0	29.0	42.0	14.0	141.2
Sm	1.5	3.1	8.3	2.9	7.7	5.8	7.0	4.0	19.3
Eu	0.67	0.98	1.80	0.79	0.98	1.10	1.80	1.20	3.91
Gd	1.8	3.5	6.2	2.2	7.5	5.2	5.6	4.3	10.4
Tb	0.29	0.58	0.80	0.30	1.20	0.87	0.68	0.71	1.07
Dy	1.7	3.3	4.3	1.5	6.6	5.3	3.8	4.4	4.8
Ho	0.35	0.68	0.83	0.30	1.40	1.10	0.70	0.90	0.72
Er	0.97	2.00	2.10	0.73	3.90	3.10	1.80	2.60	1.81
Tm	0.16	0.29	0.28	0.12	0.64	0.48	0.26	0.39	0.24
Yb	1.10	2.00	1.90	0.67	4.20	3.30	1.50	2.40	1.53
Lu	0.16	0.29	0.31	0.10	0.63	0.49	0.25	0.38	0.23
Eu/Eu^*	1.25	0.91	0.77	0.96	0.39	0.61	0.88	0.88	0.84
La_N/Yb_N	3.6	3.3	18.9	18.2	6.5	5.9	18.7	3.0	88.1
ΣREE	34.3	64.7	253.8	79.6	201.6	149.8	197.4	72.5	777.7

Table 2 (*Continued*)

Sample	H521	H117A	C196	H450	H375	H525B	P96/KC1	P96/KC2	P96/KC3
Group	2	2	2	2	2	3	3	3	3
Pluton	FG	FG	DL	CARR	H	SN	KLAC	KLAC	KLAC
Rock-type	TN	TN	MG	MG	MG	MG	JAC	IJOL	SYEN
wt. %									
SiO_2	64.9	66.2	67.7	71.0	74.8	71.8	42.5	43.4	60.3
TiO_2	0.49	0.42	0.15	0.35	0.27	0.26	1.12	0.81	0.24
Al_2O_3	14.8	15.3	16.5	14.8	13.4	14.6	7.8	15.9	15.1
FeO^T	3.60	3.15	1.44	2.70	2.34	1.62	7.41	8.67	3.63
MnO	0.07	0.05	0.03	0.03	0.02	0.03	0.11	0.13	0.09
MgO	2.51	2.05	1.09	0.79	0.67	0.49	13.68	5.47	0.73
CaO	2.74	2.83	2.17	3.43	2.35	1.59	20.21	9.57	5.23
Na_2O	5.40	4.50	5.60	4.50	3.70	4.50	1.62	6.62	6.74
K_2O	2.62	3.17	2.44	0.92	1.97	3.79	2.47	5.59	3.29
P_2O_5	0.23	0.19	0.06	0.07	0.05	0.09	3.05	0.76	0.53
LOI	2.30	1.30	0.61	0.70	0.80	0.40	na	na	na
Mg#	0.554	0.537	0.574	0.343	0.338	0.350	0.774	0.539	0.272
ppm									
Cr	59	51	3	20	10	bd	10	bd	bd
Ni	29	23	bd	bd	10	bd	23	bd	bd
Co	27	30	bd	34	5	29	na	na	na
Sc	7.0	5.6	2.0	3.3	4.7	2.3	39.0	bd	bd
V	60	49	21	24	13	14	64	95	49
Cu	bd	41	7	bd	150	bd	80	88	bd
Pb	10	20	10	5	bd	26	20	15	bd
Zn	68	47	bd	40	18	47	47	88	47
Rb	88	96	71	22	49	170	74	222	49
Ba	620	920	661	260	430	720	1092	280	756
Sr	550	730	512	230	130	520	2471	1224	832
Nb	7.0	6.9	3.5	5.2	13.0	12.0	9.2	5.7	32.1
Hf	4.0	4.2	1.8	4.0	5.3	5.4	9.8	5.2	3.1
Zr	82	140	76	123	220	129	382	258	182
Y	11	10	3	6	27	10	46	20	13
Th	8.10	6.90	4.13	3.10	9.20	19.00	14.93	8.73	7.30
U	1.70	2.30	0.98	0.29	1.60	5.20	1.78	0.71	0.64
La	42.0	41.0	22.3	26.0	37.0	73.0	232.7	89.3	77.8
Ce	94.0	85.0	40.7	51.0	71.0	140.0	592.6	238.6	205.6
Pr	11.0	10.0	4.1	5.2	7.5	15.0	83.7	34.1	26.3
Nd	42.0	38.0	13.6	18.0	28.0	49.0	353.4	144.8	94.5
Sm	6.3	6.1	1.9	2.6	4.4	6.1	57.8	24.7	13.1
Eu	1.50	1.30	0.55	0.83	0.78	1.10	13.42	6.00	2.66
Gd	3.7	3.5	1.1	1.5	4.2	2.9	34.0	14.5	7.1
Tb	0.43	0.43	0.13	0.20	0.66	0.36	3.32	1.48	0.78
Dy	2.1	1.8	0.7	1.0	4.2	1.8	13.4	6.6	3.5
Ho	0.35	0.34	0.12	0.17	0.87	0.31	1.83	0.96	0.57
Er	0.87	0.78	0.31	0.46	2.40	0.76	3.78	2.03	1.37
Tm	0.13	0.12	0.06	0.07	0.39	0.12	0.42	0.25	0.19
Yb	0.81	0.73	0.32	0.45	2.60	0.76	1.54	1.06	1.12
Lu	0.14	0.13	0.05	0.07	0.44	0.14	0.25	0.18	0.20
Eu/Eu*	0.95	0.86	1.16	1.28	0.55	0.80	0.92	0.97	0.84
La_N/Yb_N	37.2	40.3	50.0	41.4	10.2	68.9	108.4	60.4	49.8
ΣREE	205.3	189.2	85.9	107.6	164.4	291.4	1392.2	564.6	434.8

Key: CKIS = central Kaminak intrusive complex; CARR = Carr pluton; FG = Ferguson pluton; DL = Dog Lake pluton; H = Heninga pluton; SN = Snug Lake pluton; KLAC = Kaminak Lake alkaline complex; Hb DR = hornblende diorite; DR = diorite; TN = tonalite; MG = monzogranite; MZ = monzonite; JAC = jacupirangite; IJOL = ijolite; SYEN = syenite; na = not analysed; bd = below detection.

are commonly not significantly changed from their primary abundances (e.g., Whalen et al., 1999). High field strength (HFSE) and rare earth element (REE) variations typically indicate that these elements are essentially immobile under most conditions (Pearce and Cann, 1973; Wood et al., 1979; Middelburg et al., 1988; Whalen et al., 1999). We outline the major and trace element geochemistry of the plutonic rocks of the Kaminak segment of the CHSB, but emphasize their HFSE and REE variations, which we consider to largely reflect primary igneous processes.

4.2. Major and compatible trace element variations

Representative analyses from the three temporally distinct suites are presented in Table 2. All units are metaluminous (Fig. 3) with the majority, except for rare altered specimens, characterized by A/CNK ratios of $\leq$1.1 (A/CNK = molecular $Al_2O_3/Na_2O + K_2O + CaO$; adapted after Maniar and Piccoli, 1989). The rocks range from diorites and rare gabbros to granite, but are dominated by tonalite and granodiorite to less common granite (Fig. 4; Barker, 1979). Group 1 rocks are generally gabbroic to granodioritic in composition, whereas those of the group 3 are entirely granitic.

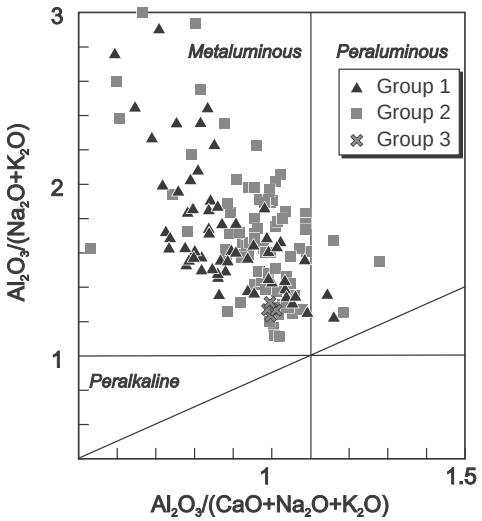

Fig. 3. Modified Shand plot (after Maniar and Piccoli, 1989) demonstrating that, with few exceptions, all plutonic rocks are metaluminous (A/CNK = molecular $Al_2O_3/CaO + Na_2O + K_2O$ < 1.1) in composition as reflected by the common presence of biotite and hornblende.

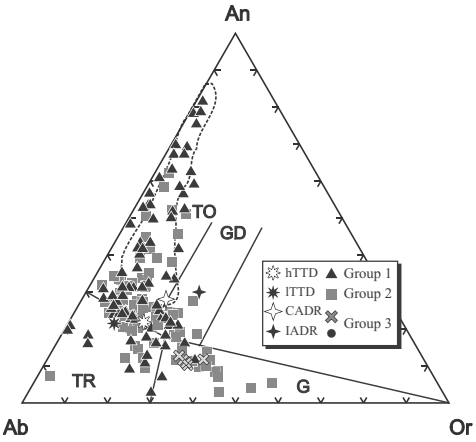

Fig. 4. Normative Ab–An–Or diagram (Barker, 1979) showing the range in compositions for plutonic rocks of the CHSB. Note that rocks of group 1 are typified by diorite and tonalite through trondjhemite with rare granite, whereas those of group 2 and 3 have more abundant granodiorite to granite. Dashed field is that for the M-type, Uasilau–Yau Yau intrusive complex of New Britain, Papua New Guinea (Whalen, 1985). Also shown are the average compositions (Drummond et al., 1996) for Archaean high-Al tonalite–trondhjemite–dacite (hTTD), low-Al tonalite–trondhjemite–dacite (lTTD), island arc andesite–dacite–rhyolite (IADR) and calc-alkaline andesite–dacite rhyolite (CADR). Key: G = granite; TR = trondjhemite; GD = granodiorite and; TO = tonalite to gabbro.

Rocks of group 1 are low- to medium-K_2O, as are the majority of rocks from group 2 (Fig. 5); however, K_2O increases significantly at higher SiO_2 values amongst group 2. All the rocks from group 3 are high-K_2O monzogranites or, alternatively syenites and associated alkalic rocks. In a molecular Na–K–Ca plot (Fig. 6), granitoids of group 1 exhibit minimal K_2O enrichment relative to those of group 2, and have a similar trend to rocks of the M-type, Uasilau–Yau Yau intrusive complex of New Britain, Papua New Guinea (Whalen, 1985). Group 1 rocks also trend towards the field of the tonalite–trondjhemite–granite (TTG) suite (Arth and Barker, 1976; Barker and Arth, 1976; Martin, 1995). In contrast, group 2 granitoids exhibit a K_2O enrichment similar to that of modern, calc-alkaline plutons (Barker and Arth, op. cit.). The majority of the granitoid rocks are calc-alkaline as demonstrated by their lack of iron enrichment trends on the AFM diagram of Irvine and Barager (1971). Gabbroic to dioritic rocks of both groups 1 and 2, however, exhibit both calc-alkaline and tholeiitic affinities (Fig. 7).

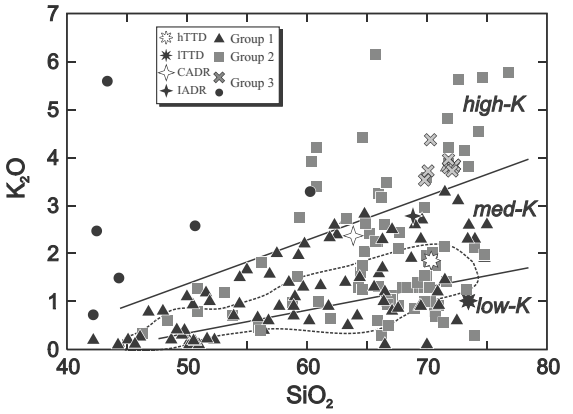

Fig. 5. K_2O vs. SiO_2 diagram (after Le Maitre, 1989) for plutonic units of the CHSB. Note that rocks of group 1 are typified by low- and medium-K_2O whereas those of groups 2 and 3 range to high-K_2O compositions. Also shown are the samples from the Kaminak Lake alkaline complex (solid dots) comprising jacupirangite, ijolite and syenite. All remaining symbols and fields are as in Fig. 4.

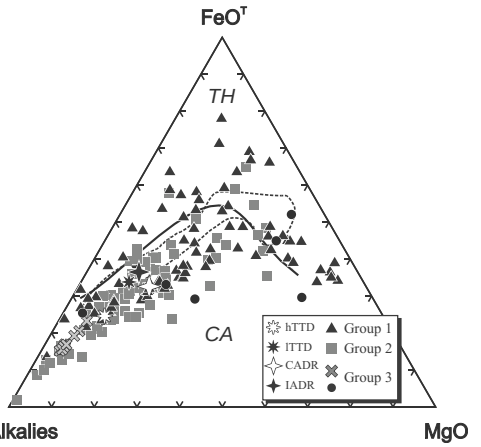

Fig. 7. Plot of alkalis-FeO^T (total iron as ferrous iron)-MgO for plutonic rocks of the CHSB (after Irvine and Barager, 1971). CA and TH represent the calc-alkaline and tholeiitic fields, respectively. All remaining symbols and fields are as in Fig. 4.

Granitoid rocks from all three groups exhibit marked variation in major and trace element contents relative to SiO_2. Harker variation diagrams for Al_2O_3 and Mg# (molecular MgO/MgO + FeO^T; Fig. 8) indicate great variability. For example, mafic rocks of group 1 have highly variable Al_2O_3 contents (12–22 wt.%) and Mg#'s (0.26–0.74) over a narrow SiO_2 range of 45–50 wt. %. This implies that all of these mafic rocks are unlikely to be related through any simple petrogenetic process. A similar conclusion may be drawn from the major element variations of the group 2 mafic rocks. These features are not unexpected in view of the fact that both groups are characterized by tholeiitic and calc-alkaline mafic suites. Except at SiO_2 > 60 wt.%, rocks of groups 1 and 2 exhibit Al_2O_3 concentrations lower than comparable M-type granitoids of the New Britain area (Whalen, 1985) and have higher Mg#'s. This suggests that the source of the majority of the plutonic rocks of the CHSB may have been significantly more magnesian than that for most Phanerozoic granitoids, even those interpreted as having been ultimately derived from a large proportion of asthenospheric mantle (cf. Whalen, 1985). Alternatively, these Neoarchaean rocks may have resulted from higher degrees of partial melting than Phanerozoic equivalents.

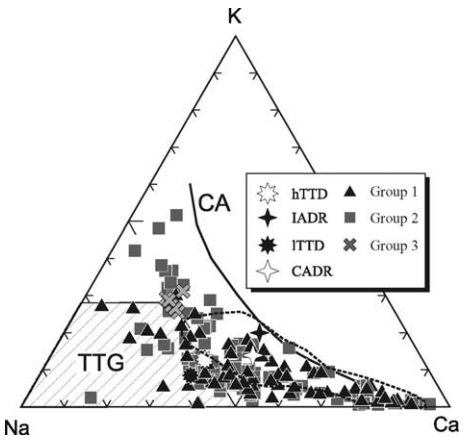

Fig. 6. Molecular Na–K–Ca plot for plutonic rocks of the CHSB. Hatched box represents the field for Archaean TTG suites and CA represents the calc-alkaline trend (Martin, 1995). All remaining symbols and fields are as in Fig. 4.

4.3. REE and multi-element patterns

Figs. 9–11 show chondrite normalised rare earth element diagrams and multi-element profiles normalized to primitive mantle (PM; Sun and McDonough, 1989) for each of the three plutonic groups. Salient petrochemical features and U–Pb ages are given in Tables 1 and 2. Analyses shown in the diagrams are divided into mafic (≤56 wt.% SiO_2), intermediate (>56 and

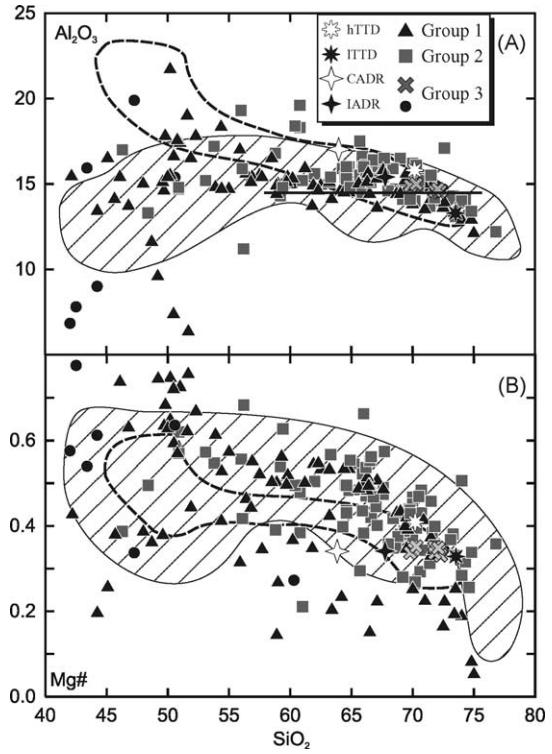

Fig. 8. Harker variation diagrams for plutonic rocks of the CHSB (A) Al_2O_3 vs. SiO_2 (B) Mg# vs. SiO_2. Horizontal solid line divides high- and low-alumina Archaean TTG suites (Arth, 1979) whereas the diagonally ruled field is that for 145 volcanic rocks of the CHSB (Sandeman et al., 2004). Dashed field is that for the M-type, Uasilau–Yau Yau intrusive complex of New Britain, Papua New Guinea (Whalen, 1985).

<70 wt.% SiO_2) and felsic (≥70 wt.% SiO_2) units based on their bulk-rock SiO_2 in conjunction with their total-alkali elements contents (LeBas et al., 1986).

4.3.1. Group 1 plutons

Group 1 mafic rocks exhibit a wide range of incompatible element abundances (Fig. 9A), presumably reflecting their more variable major and compatible trace element variations relative to the other groups. The samples comprise two sub-groups, one exhibiting generally flat and the other having LREE enriched REE profiles. The former have variable, but commonly positive Eu anomalies (Taylor and McLennan, 1985), and overall low abundances of the REE's (Tables 1 and 2). Their multi-element profiles exhibit minor but variable negative Nb, P and Zr troughs, but have variable but generally positive Sr, Eu and Ti anomalies indicative of plagioclase and possibly magnetite accumulation (Fig. 9B). The second sub-group is characterized by stronger LREE-enrichment, variable but generally negative Nb, P and Ti troughs and variable Eu and Sr anomalies.

Group 1 intermediate rocks are remarkably similar in terms of their REE and multi-element profiles, with moderately fractionated REE patterns (Fig. 9C; Tables 1 and 2), negligible to very minor, positive and negative Eu anomalies and moderate abundances of the REE (Fig. 9D). These rocks have profiles showing prominent negative Nb, P and Ti troughs with variable negative Sr anomalies.

The trace element composition of one group 1 felsic rock closely resembles those of the rocks of intermediate composition described above. The remaining felsic samples exhibit less fractionated patterns with variable negative Eu troughs and flat HREE profiles (Fig. 9E). Overall, their LREE abundances resemble those of the intermediate units, but they have slightly higher average HREE abundances (Tables 1 and 2). Their multi-element profiles are parallel, exhibiting significant negative troughs for Nb, Sr, P, Ti and also for Eu (Fig. 9F).

4.3.2. Group 2 plutonic rocks

Group 2 mafic rocks exhibit variable REE patterns ranging from non-fractionated, flat patterns having modest positive Eu anomalies to fractionated REE profiles with negligible Eu anomalies (Tables 1 and 2; Fig. 10A). Overall, the LREE abundances are highly variable, and these rocks have similarly variable multi-element profiles ranging from non-fractionated cumulate samples having positive Sr and Ti troughs, to fractionated patterns characterised by negative Nb, Sr, P, Ti and Eu anomalies (Fig. 10B).

With the exception of the Carr Lake monzonite (see below), all rocks of intermediate composition have similar REE and multi-element profiles. The patterns are steep, have both minor negative and positive Eu anomalies, and have concave HREE segments (Tables 1 and 2; Fig. 10C). The multi-element profiles are parallel and exhibit prominent negative anomalies for Nb, P and Ti, and variably negative Sr anomalies (Fig. 10D). Samples of the Carr monzonite are enriched in the REE, exhibit very strongly fractionated patterns and have negligible negative Eu anomalies

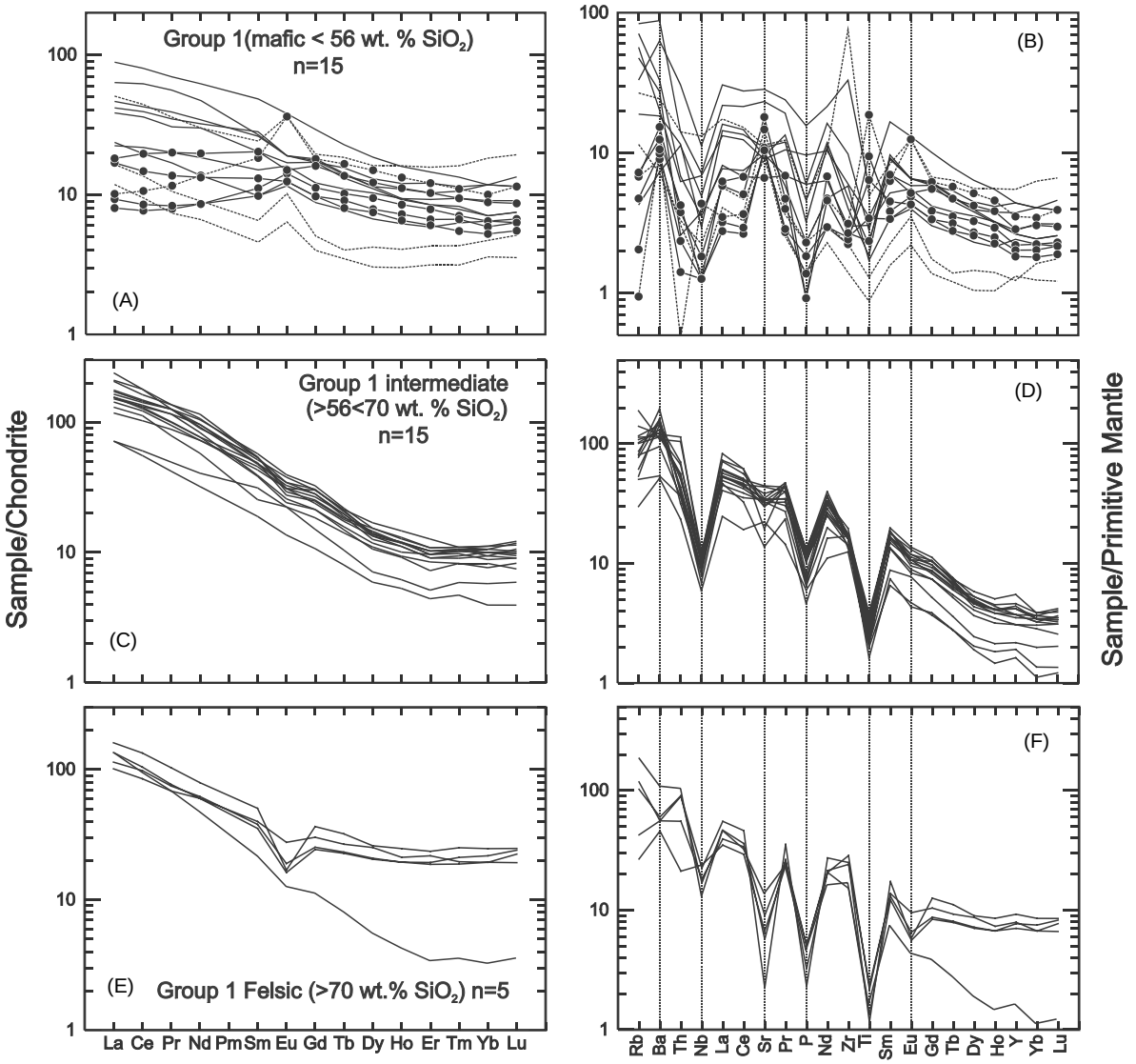

Fig. 9. Rare earth element and multi-element plots (normalization after Sun and McDonough, 1989) for rocks of group 1. (A, B) mafic rocks; (C, D) intermediate rocks; (E, F) felsic rocks. Dashed patterns in (A) and (B) are specimens exhibiting high abundances of MgO, Cr, Ni, Sr or Eu implying that they comprise a large proportion of cumulate phases. The sub-group of samples having flat REE patterns are shown by the patterns with black dots.

(Tables 1 and 2). Their multi-element profiles resemble those described above, but with higher LREE and lower HREE contents.

Felsic rocks exhibit a wide range of REE and multi-element profiles. With two exceptions (see below), the REE profiles define a continuous range in the degree of fractionation, a feature most strongly outlined by the variations in the HREE rather than LREE concentrations (Fig. 10E). The most fractionated patterns resemble the intermediate rocks (see above) whereas those with less fractionated patterns are comparable to the felsic granitoids of group 1 (cf. Fig. 9E). Most specimens exhibit variable negative Eu anomalies and have moderate abundances of the REE, except for one possible cumulate with a positive Eu anomaly. Felsic rocks of group 2 have

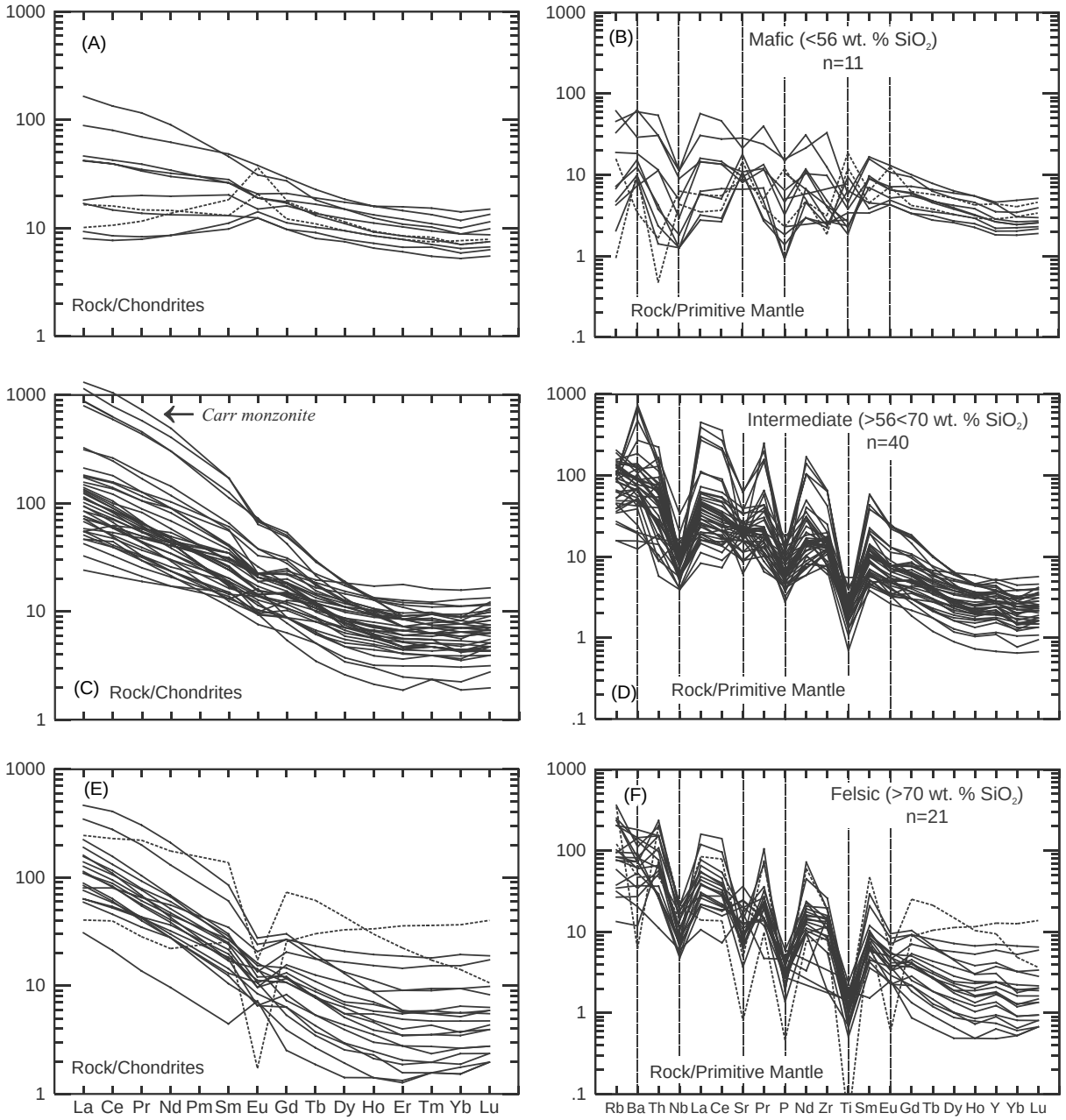

Fig. 10. Rare earth element and multi-element plots (normalization after Sun and McDonough, 1989) for rocks of group 2. (A, B) mafic rocks; (C, D) intermediate rocks; (E, F) felsic rocks. Dashed patterns in (A) and (B) are specimens exhibiting high abundances of MgO, Cr, Ni, Sr or Eu implying that they comprise a large proportion of cumulate phases. Dashed patterns in (E) and (F) are from highly fractionated, late syenogranitic dykes marginal to the Carr Pluton.

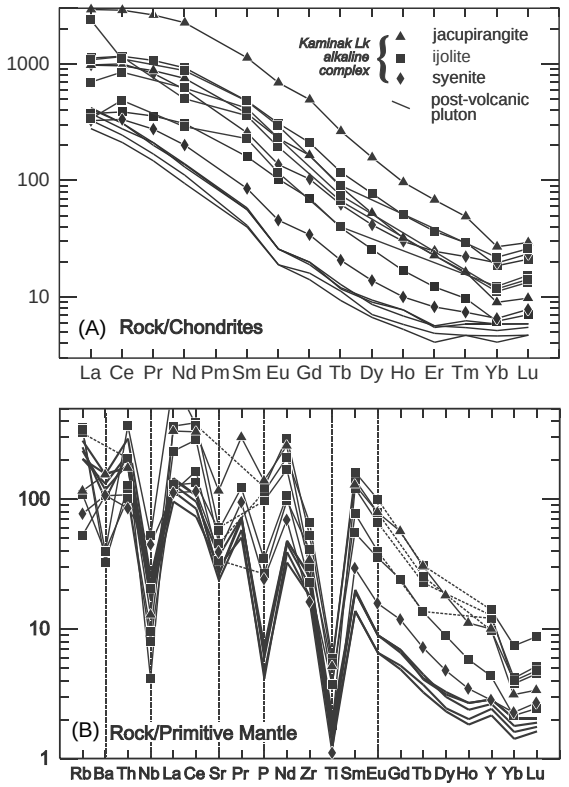

Fig. 11. (A) Rare earth element and (B) multi-element plots for rocks of the group 3 Snug Lake pluton (solid lines) and the Kaminak Lake alkaline complex (lines with symbols; normalization after Sun and McDonough, 1989).

prominent negative Nb, P and Ti anomalies, and increasing HREE abundance is correlated with the magnitude of their Eu and Sr troughs (Fig. 10F). Two specimens, obtained from veins cross-cutting adjacent host rocks, exhibit anomalous REE and multi-element profiles. These are shown as dashed lines in Fig. 10E. These two specimens exhibit convex-down and convex-up REE profiles and have relatively unfractionated patterns with strong negative Eu anomalies.

4.3.3. Group 3 plutonic rocks

The monzogranitic Snug Lake pluton has LREE-enriched, strongly fractionated REE profiles with minor negative Eu troughs (Tables 1 and 2) and coherent multi-element profiles having pronounced negative Nb, Sr, P and Ti anomalies and minor troughs for Ba and Eu (Fig. 11A and B). These rocks have, overall, high abundances of the REE and incompatible elements.

Representative specimens from the jacupirangite, ijolite and syenite of the Kaminak alkaline complex (Davidson, 1968, 1970b; Irwin, 1994) are LREE-enriched and have fractionated REE profiles lacking Eu anomalies (Tables 1 and 2). The LREE patterns are distinctively convex (Fig. 11A) and their multi-element profiles have pronounced negative Nb, Sr, P and Ti anomalies and variable Ba troughs (Fig. 11B).

4.4. Nd isotopic data

In view of the small (≤20 m.y.; Davis et al., in press) difference in age, initial $^{143}Nd/^{144}Nd$ and $\in Nd_t$ values presented in Table 3 (after DePaolo, 1981) are calculated at 2690 Ma for the rocks of groups 1 and 2, whereas those for group 3 rocks are calculated at 2666 Ma. All rocks of groups 1 and 2, including duplicates, yield present day $^{143}Nd/^{144}Nd$ ratios ranging from 0.510743 to 0.511846 with corresponding $\in Nd_{t=2690\,Ma}$ values of +1.2 to +3.3 (mean = +2.2; $n = 14$), overlapping (within error) with the value for contemporaneous depleted mantle ($\in Nd_{t=2690\,Ma} = +2.2$). Present day $^{143}Nd/^{144}Nd$ ratios for the group 3 rocks range from 0.510608 to 0.510660 with corresponding $\in Nd_{t=2666\,Ma}$ values of +1.4 to +2.3 (mean = +2.0; $n = 4$), also overlapping with depleted mantle values. T_{DM} ages (time of removal from depleted mantle; DePaolo, 1981) range from 2589 to 2795 Ma (mean = 2709 Ma), implying that most of the intrusive rocks were derived from the mantle, or juvenile crustal rocks.

In Fig. 12, we plot $\in Nd_t$ versus time for the granitoids of the CHSB and compare these to the range of values for 7 felsic and 23 mafic volcanic rocks from the region (Sandeman et al., 2004). The granitoids have less variable $\in Nd_t$ than both the felsic and mafic volcanic rocks, although the mean $\in Nd_t$ values for all three are essentially identical within error. The Nd isotopic data indicate that all of these rocks were derived from direct partial melting of the mantle or, alternatively, crustal sources that had short crustal residence times. There is no evidence for reworking of significantly older continental crust, but some group 2 specimens with $\in Nd_t$ values below ca. +1.8 may have experienced minor

Table 3
Nd isotopic data for plutonic units of the CHSB

Sample	Unit	Rock-type	Age (Ma)	Sm (ppm)	Nd (ppm)	$^{147}Sm/^{144}Nd$ measured	$^{143}Nd/^{144}Nd$ measured	∈Nd (T)	T_{DM} (Ma)
Group 1									
PHA97H33A	CKIS	Diorite	2691	16.38	69.42	0.1426	0.511846 ± 6	3.29	2589
PHA97H25A	CKIS	Monzogranite	2691	7.64	37.53	0.1230	0.511446 ± 5	2.29	2708
PHA97P610	CKIS	Diorite	2691	7.27	30.65	0.1433	0.511775 ± 11	1.67	2778
PHA97P610*	CKIS	Diorite	2691	1.48	6.25	0.1433	0.511818 ± 7	2.51	2679
Group 2									
PHA97H61A	Carr	Monzonite	2681	92.89	677.08	0.0829	0.510776 ± 6	2.90	2660
PHA97H110A	Ferguson	Quartz diorite	2679	21.73	92.94	0.1413	0.511789 ± 5	2.63	2667
PHA97H161	Kaminak	Tonalite	2679	19.29	112.08	0.1040	0.511067 ± 8	1.46	2770
PHA97H512A	Carr	Tonalite	2679	1.64	11.77	0.0840	0.510777 ± 7	2.73	2682
PHA97H512A*	Carr	Tonalite	2679	8.13	58.46	0.0841	0.510743 ± 5	1.74	2725
PHA97C196	Dog Lake	Tonalite	2679	1.87	13.44	0.0839	0.510778 ± 10	2.77	2680
PHA97H375	Heninga	Tonalite	2679	4.55	25.24	0.1089	0.511139 ± 11	1.18	2795
PHA97H521	Ferguson	Tonalite	2679	5.88	37.54	0.0946	0.510925 ± 7	1.94	2733
PHA97H298A	Carr	Tonalite	2688	2.77	15.40	0.1086	0.511171 ± 13	1.91	2738
PHA97124	Carr	Quartz diorite	2688	7.04	39.82	0.1069	0.511153 ± 9	2.15	2719
Group 3									
PHA97H525	Snug	Monzogranite	2666	5.29	41.13	0.0778	0.510660 ± 7	2.25	2691
PHA97H525*	Snug	Monzogranite	2666	5.57	42.97	0.0783	0.510626 ± 18	1.39	2742
PHA97H497	Snug	Monzogranite	2666	5.84	46.11	0.0766	0.510641 ± 2	2.29	2689
PHA97H508A	Snug	Monzogranite	2666	6.21	49.61	0.0757	0.510608 ± 3	1.95	2708

Key: Units refer to plutons or intrusive complexes shown in Fig. 2. T_{DM} age calculated after DePaolo (1981). Asterisks designate duplicate samples. All Nd values calculated to $t = 2690$ Ma.

amounts of contamination by an older, evolved crustal source.

5. Discussion

Any tectonomagmatic model for generation of the CHSB must account for the following field and lithogeochemical features of the contained granitoids:

(1) The bulk of the CHSB was formed over a short interval (2711–2679 Ma): group 3 plutonic rocks (younger than 2679 Ma) are rare and comprise potassic biotite monzogranites or strongly alkaline intrusions that are dissimilar to earlier rocks.
(2) Two volcanic and two major plutonic cycles are present: mafic and felsic units (both volcanic and plutonic) are temporally and spatially associated throughout.
(3) Mafic plutonic rocks are more abundant in early plutonism, whereas intermediate to felsic intrusions dominate the middle and latter stages.
(4) Group 2 tonalites and granodiorites are the most voluminous.
(5) The three plutonic associations (groups 1–3) are metaluminous, I- or M-type granitoids, dominated by intermediate compositions, and exhibit an overall increase in incompatible trace elements with time.
(6) Many granitoids of the CHSB exhibit Mg#'s that are similar to, or greater than, the cogenetic volcanic rocks that they intrude.
(7) Groups 1 and 2 comprise both tholeiitic and calc-alkaline rocks that cannot be linked through any simple petrogenetic model.
(8) $\in Nd_t$ values for representative samples of all groups overlap, within error, with that for contemporaneous depleted mantle.
(9) The short time interval between the emplacement of rocks of group 1 versus group 2, and marked changes in the compositional character of both the plutonic and volcanic rocks at ca. 2688 Ma, imply a significant change in the tectonic environment(s).

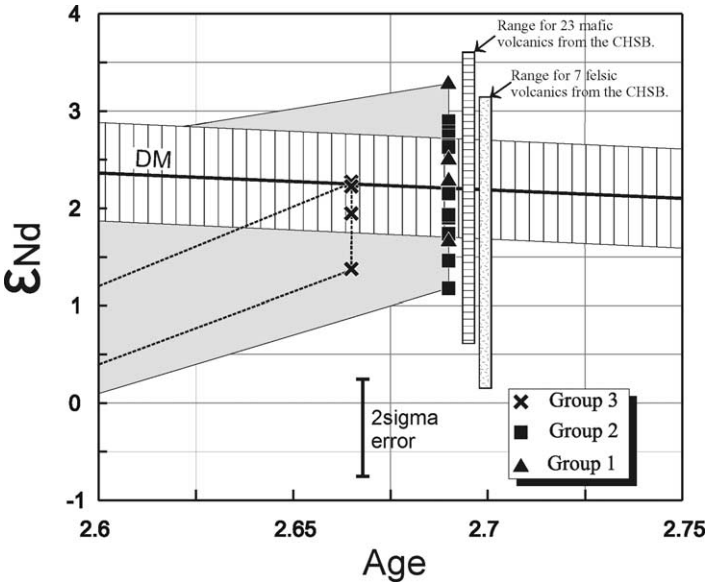

Fig. 12. $\in Nd_{t=2690\,Ma}$ vs. time for 12 specimens (+2 duplicates) of plutonic rocks from the CHSB, including those from both groups 1 and 2. These are compared to ranges for 23 mafic and 7 felsic volcanic rocks from the CHSB (Sandeman et al., 2004). Also shown are $\in Nd_{t=2666\,Ma}$ for three samples and one duplicate from the group 3, Snug Lake pluton. $\in$Nd results are calculated using the parameters of Jacobsen and Wasserburg (1980) ($^{143}Nd/^{144}Nd_{0(CHUR)} = 0.512638$; $^{147}Sm/^{144}Nd_{(CHUR)} = 0.1967$). The depleted mantle curve was calculated according to the parameters of DePaolo (1981).

In light of the salient field, geochemical and geochronological observations for the plutonic and volcanic sequences of the CHSB as addressed herein and in accompanying contributions (Hanmer et al., in press; Davis et al., in press; Sandeman et al., 2004), below we provide, what we consider, to represent the most actualistic model for the formation and evolution of the central Hearne lithosphere. Our account does not emphasize the necessity to generate TTG suites in either thick lower crust (cf. Kamber et al., 2002 and references therein) or a foundered slab (Drummond et al., 1996 and references therein), but in particular, focuses on the integration of all available field, geochronological and petrological data for the region.

5.1. Classification, tectonomagmatic setting and incompatible element variations

Except for the most mafic examples, and radically alkaline units, all the granitoids of the CHSB are biotite ± hornblende-bearing and represent metaluminous, I- or M-type granitoids. The majority of the granitoids are sodic rather than potassic (except for high SiO_2 examples) and have high but variable Al_2O_3 contents. About half of both group 1 and 2 plutons are notably depleted in K_2O, LILE, HFSE and exhibit Rb/Sr $\leq$0.20, features typical of largely mantle-derived, M-type plutonic rocks of juvenile, intraoceanic island arcs (Whalen, 1985). In the trace element tectonomagmatic discrimination diagrams of Pearce et al. (1984, not shown), virtually all granitoids of the CHSB plot as volcanic arc granites.

The plutonic rocks exhibit a wide range in their incompatible element abundances. In particular, they have variable, but apparently gradational degrees of LIL and LREE enrichment as shown by their REE and multi-element patterns (Figs. 8–10). They show both HREE-enriched and HREE-depleted REE patterns, indicating that many resemble other Archaean, low- and high-Al_2O_3 tonalite–trondhjemite–granodiorite suites (TTG or TTD; Arth and Barker, 1976; Martin, 1986, 1995), respectively. Chondrite normalized La/Yb (La_N/Yb_N; Table 2) is useful in distinguishing the degree of fractionation. La-poor rocks (i.e., $La_N/Yb_N < 12$) correspond to tholeiitic rocks from both groups 1 and 2. La-rich rocks (La_N/Yb_N

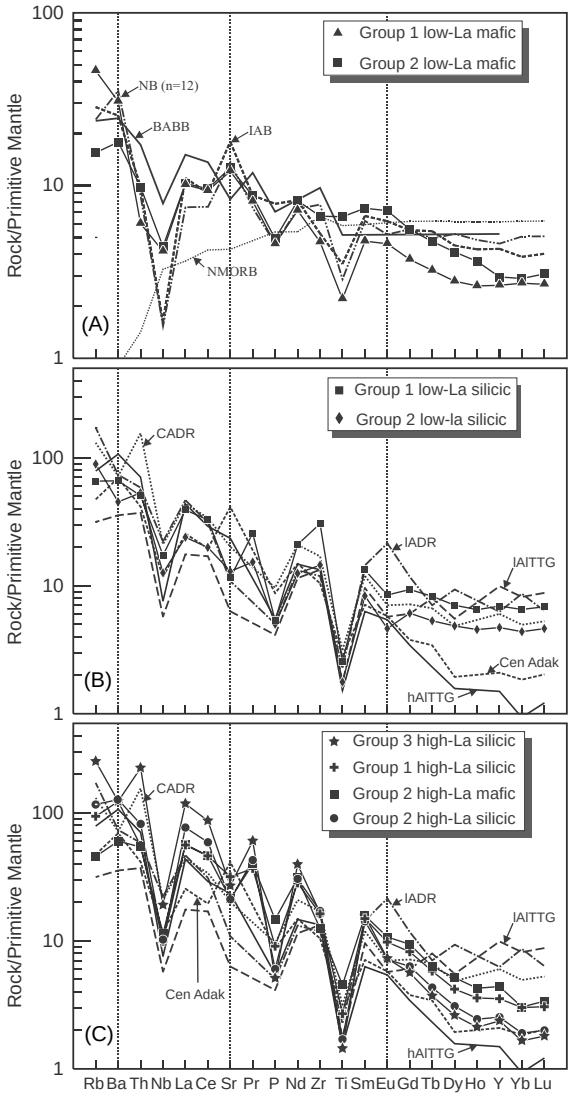

Fig. 13. (A) Multi-element plots for average low La_N/Yb_N mafic rocks from groups 1 and 2 compared to patterns for modern-day island arc basalt (IAB; Pearce, 1982), normal mid-ocean ridge basalt (NMORB; Sun and McDonough, 1989), back-arc basin basalts (BABB; Saunders and Tarney, 1991) and plutonic rocks of the New Britain arc (NB; Whalen, 1985). (B) Multi-element plots for average low La_N/Yb_N felsic rocks of groups 1 and 2 compared to patterns for calc-alkaline andesite–dacite–rhyolite (CADR), island arc andesite–dacite–rhyolite (IADR), Cenozoic adakites (Cen Adak), low alumina tonalite-trondhjemite-granite (lAlTTG) and high alumina tonalite-trondhjemite-granite (hAlTTG). (C) Multi-element plots for average high La_N/Yb_N felsic rocks of groups 1–3 compared to patterns for calc-alkaline andesite–dacite–rhyolite (CADR), island arc andesite-dacite-rhyolite (IADR), Cenozoic adakites (Cen Adak), low alumina tonalite-trondhjemite-granite (lAlTTG) and high alumina tonalite–trondhjemite–granite (hAlTTG). Average compositions for the comparative rock-types are from Drummond et al. (1996).

> 12) occur in both groups 1 and 2 but are more abundant in group 2. All group 3 rocks are La-rich.

Mafic ($\leq$55 wt.% SiO_2) and intermediate to felsic (>55 wt.% SiO_2), La-poor rocks from both groups 1 and 2 are most similar to depleted island arc tholeiites or island arc andesite–dacite–rhyolite suites (IAB or IADR) and continental arc andesite–dacite–rhyolite suites (CADR; Fig. 13A and B), respectively. However, the average composition for low-La rocks from the study area has lower HREE abundances than rocks from modern intra-oceanic arcs (Fig. 13A and B). These differences may arise through relatively low-*P*, dry crustal melting and fractionation conditions accompanied by removal of plagioclase, clinopyroxene and magnetite (Whalen, 1985; Drummond et al., 1996). The somewhat lower abundances of the HREE in mafic rocks of groups 1 and 2 as compared to modern ADR suites likely signifies the participation of hornblende or possibly minor garnet during melting reactions in the source, or fractionation during ascent (Hanson, 1978; Arth, 1979).

In contrast, La-rich plutonic rocks of all three groups and of both mafic and felsic composition, most closely resemble high Al_2O_3 TTG suites and also Cenozoic adakites (Cen Adak; Fig. 13C). Adakites have positive Sr and negligible Ba anomalies, in contrast with the patterns shown by felsic plutonic rocks of groups 1 and 2. These observations suggest, therefore, that the parental magmas of the La-rich, group 1 and 2 granitoids fractionated plagioclase, but apparently not biotite or potassium feldspar. This suggestion is supported by petrographic observations (ubiquitous rare and paragenetically late oikocrystic microcline) and the presence of small negative Eu anomalies in their REE patterns. If the amount of fractional crystallization was minimal, then these elemental relationships might be easily explained through partial melting of a biotite absent, amphibolitic or eclogitic source. Group 3 felsic granitoids most closely resemble continental ADR rocks, but have higher overall abundances of the LIL and LREE and much lower abundances of the HREE. These

points suggest that the group 3 rocks, like the groups 1 and 2, La-rich felsic rocks, represent partial melts of a garnet + hornblende + plagioclase-bearing mafic source in a tectonic setting characterized by elevated geotherms. In contrast to the groups 1 and 2 felsic rocks, the negative Ba, Sr and Eu anomalies exhibited by the group 3 granitoids imply that these have undergone late fractional crystallization of plagioclase and probably potassium feldspar or biotite (Hanson, 1978).

The highly evolved rocks of the Kaminak Lake alkaline complex (Fig. 11C) resemble other documented Archaean alkaline complexes (cf. Villeneuve and Relf, 1998) and are interpreted to represent very low-degree partial melts of metasomatically enriched lithospheric mantle.

5.2. Implications of isotopic data

Time corrected ∈Nd values for 15 plutonic rocks from the CHSB (and four duplicates) range from +1.1 to +3.2 (mean = +2.2) and overlap with the value for contemporaneous depleted mantle. Davis et al. (in press) and Sandeman et al. (2004) argue that any contamination of the primary magmas yielding the volcanic rocks of the CHSB likely occurred in their mantle source rather than during ascent through the crust. Because the Neoarchaean plutonic rocks of the region also have juvenile Nd isotopic compositions, it is also probable that any contamination of the primary magmas yielding these intrusive rocks occurred in their mantle source. Thus, the source of the rapidly formed, isotopically juvenile crust of the Central Hearne domain was likely depleted asthenospheric mantle with perhaps a minor component of subducted sediment.

5.3. Constraints on the source components

The similarity of the major, trace and Nd isotopic compositions of the granitoids of the region to those produced at modern destructive plate margins suggests that the CHSB plutonic rocks likely formed in an environment characterized by comparable tectonomagmatic processes. Possible source materials involved in the petrogenesis of granitoids formed at such juvenile plate margins include: (1) mantle materials, including LILE-enriched mantle wedge and MORB-type sources, followed by fractional crystallization at lower pressures, (2) subducted materials, comprising oceanic lithosphere and pelagic and/or clastic sediments, and (3) an overriding plate, including juvenile oceanic crust and/or older continental material. The juvenile nature of all of the igneous rocks and an absence of geochronological inheritance in U–Pb studies (Cavell et al., 1992; Davis et al., in press) indicates that interaction with significantly older continental material was not significant. The predominant arc-like major and trace element geochemistry in conjunction with characteristic HFSE troughs exhibited by granitoids of Archaean belts is commonly attributed to generation of such rocks in convergent plate margin settings (Pearce, 1982; Pearce et al., 1984).

Plots of La_N/Yb_N versus Yb_N and Sr/Y versus Y (Fig. 14A and B) have been widely used to discriminate between classical island arc granitoids and adakites (Drummond and Defant, 1990; Whalen et al., 1999). The enrichment of La_N/Yb_N or Sr/Y is a function of melting within the stability field of garnet, whereas the enrichment of Yb_N or Y implies melting outside of the garnet stability field. These diagrams demonstrate that ca. 60% of group 1 and ca. 27% of the group 2 granitoids are most compatible with an origin through partial melting outside of the garnet stability field ($P \leq 1.5$ GPa; <50 Km). All remaining granitoid rocks have La_N/Yb_N and Sr/Y comparable to adakites and likely had garnet in their source. This suggests that they were generated under *P–T* conditions of 1.5–2.0 GPa and 850–1150 °C (Sen and Dunn, 1994; Rapp et al., 1999).

6. Evolving geotectonic setting

Although numerous models have been proposed for the origin of Archaean supracrustal belts and associated plutonic rocks, such models have generated greater debate regarding the extent to which modern plate tectonics are applicable to early Earth history. Proposals ranging from oceanic sags to continental basins, island arcs to marginal basins, ocean ridge to plume-related oceanic plateaux, and accretionary to vertical tectonics (e.g., Choukroune et al., 1997; de Wit and Ashwal, 1997; Hamilton, 1998) are commonly debated, yet none of these uniquely satisfy the

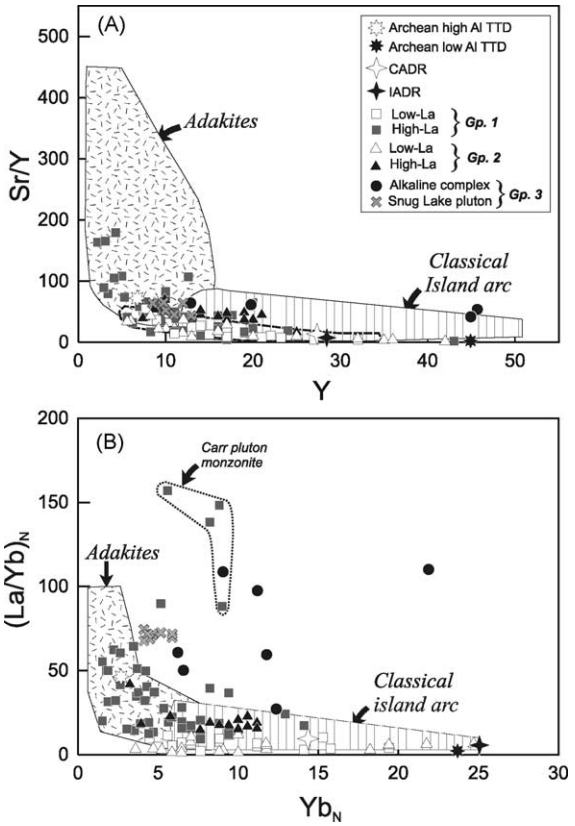

Fig. 14. (A) Plot of Sr/Y vs. Y for plutonic rocks of the CHSB (after Drummond and Defant, 1990). (B) Plot of La_N/Yb_N vs. Yb_N for plutonic rocks of the CHSB (after Drummond and Defant, 1990). Four specimens of the LREE-enriched Carr pluton monzonite are outlined by the dotted field.

geological, geochronological and petrochemical features of the CHSB.

In our companion papers (Hanmer et al., in press; Sandeman et al., 2004; Davis et al., in press), we suggest that the intimate primary intercalation of petrogenetically diverse mafic to felsic volcanic rocks throughout the magmatic history of the CHSB, the scale of the swath of juvenile crust over which this diversity is contemporaneously developed, and the lack of lateral temporal polarity are incompatible with either development of a classical volcanic arc above a subduction zone, or formation of an oceanic plateau, classically associated with an intraoceanic hot-spot or plume. Moreover, the scarcity of plume-related, high MgO volcanic suites (komatiites) implies that unlike many Archaean greenstone belts (e.g., Tomlinson and Condie, 2001; Ayer et al., 2002; Wyman et al., 2002; Scott et al., 2002), the CHSB probably did not form in association with an active mantle plume.

Thus, we have shown that the granitoid rocks of the CHSB comprise three major groups, the first two of which are correlative with volcanic assemblages 1 and 2, respectively. Group 3 plutonic rocks are post-tectonic and lack volcanic equivalents. The three groups have compositional characteristics indicating that they were generated in a juvenile, subduction zone setting. The bulk compositions of group 1 rocks are analogous to: modern arc granitoids resulting from direct partial melting of recently LILE-fluxed, depleted asthenospheric mantle (IAT or IADR source), or from anatexis of mafic lower to middle crust with variable amounts of garnet in the source (garnet amphibolite to eclogite) (Smithies, 2000; Petford and Gallagher, 2001). Groups 2 and 3 granitoids were likely derived from higher-*P* anatexis of a downgoing, eclogitic oceanic slab (Drummond and Defant, 1990; Drummond et al., 1996; Martin, 1999) or, as proposed by Kamber et al. (2002) from direct partial melting of recently LILE-fluxed, depleted asthenospheric mantle (IAT or IADR source). The major distinction between these two possible scenarios is fundamentally the depth of partial melting. Although the thickness of oceanic crust in the Archaean is poorly known, and at most a hypothetical projection, arguments have been levied that suggest it may have been thicker than at present, ranging up to 40 km (e.g., Nisbet and Fowler, 1983; Abbott et al., 1994; de Wit and Ashwal, 1997). This would indicate that throughout much of the magmatic history of the CHSB, granitoids were emplaced into relatively thick, juvenile crust.

Fig. 15 presents a series of interpretive diagrams that speculate on the relative roles of plausible source materials in the genesis of the volcanic and granitoid rocks of the CHSB. We draw attention to the types of processes invoked to explain the infant-arc (proto-arc) stage of growth of the SW Pacific Ocean (Stern and Bloomer, 1992; Bloomer et al., 1995) during the Eocene, which preceded development of volcanic arcs above subduction zones (Fig. 15). These processes include subsidence of a lower plate in front of the leading edge of an upper plate that is extended over a width measured in 100's of kilometers and pulled apart into fault-bounded extensional basins. Subsidence controls the locus of voluminous magmatism,

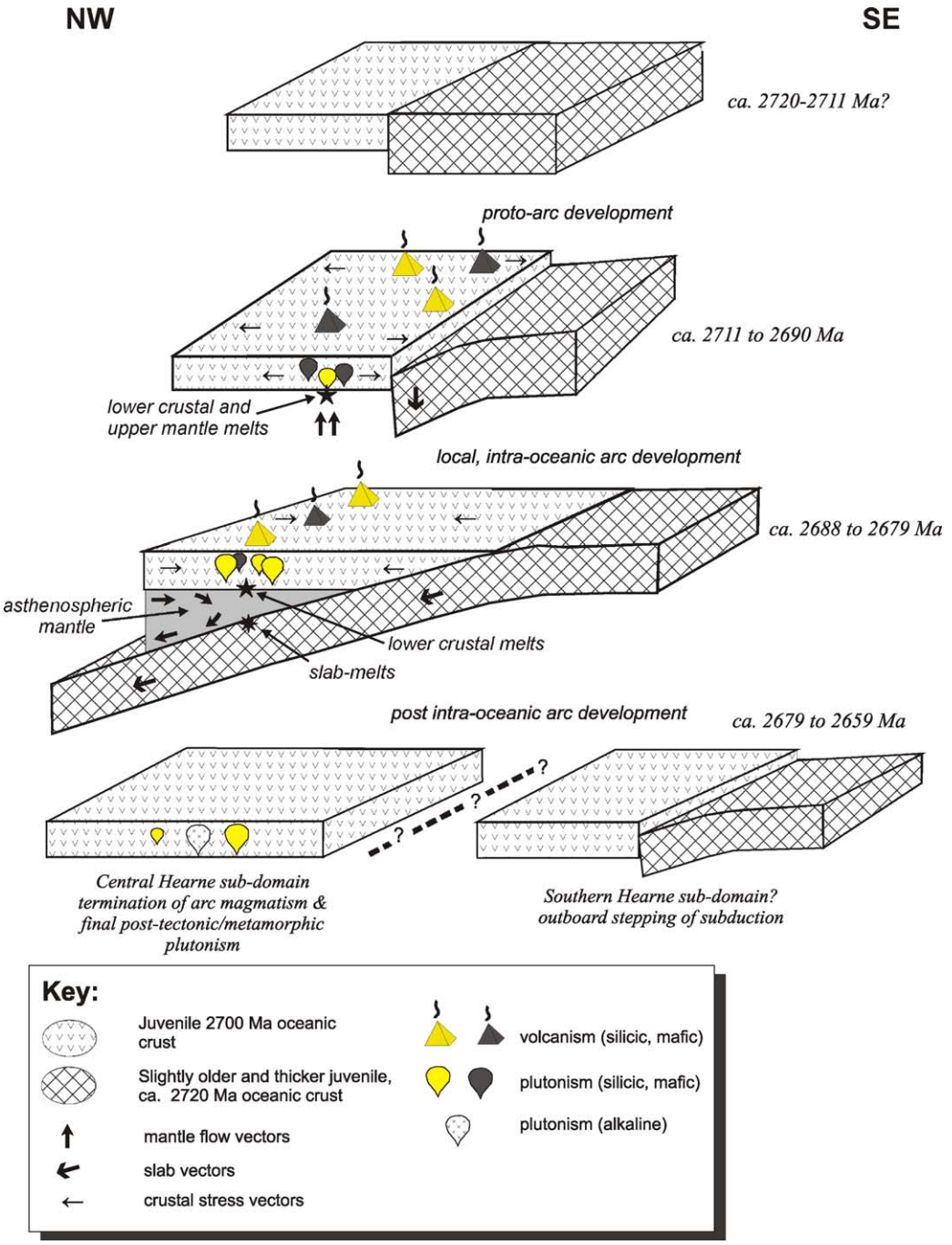

Fig. 15. Schematic diagram showing the temporal evolution of the CHSB with particular emphasis on the compositional evolution of plutonic units.

driven by return flow of hot asthenospheric material displaced by the subsiding slab. The infant arc model is, however, most readily applicable only to volcanic assemblage I (~2711–2690 Ma) and group 1 plutons that were locally deformed prior to emplacement of volcanic assemblage II (~2685–2680 Ma) and their contemporaneous group 2 plutons. An increase in the proportion of felsic volcanic rocks and a "bloom" of intermediate to felsic plutons suggests a change in tectonic environment at ~2688–2685 Ma. Thus, a change in the composition of the constituent granitoids and therefore a change in the geodynamic setting of formation of the belt is indicated.

The role of, and indeed the presence of pre-exisiting oceanic lithosphere is, however, difficult to establish because of the absence of rocks amenable to U–Pb dating techniques. Hence, we acknowledge that large tracts of homogeneous, undated, MORB-like basaltic rocks in the CHSB (e.g., immediately north of Quartzite Lake; Fig. 2) may represent currently unrecognized and slightly older "oceanic basement" material that would be difficult to recognize with Nd isotopes. Nevertheless, according to our working hypothesis, extension in the overriding plate led to the creation of a broad swath of juvenile, compositionally diverse proto-arc crust, including mafic and felsic volcanic rocks of volcanic assemblage I, that was intruded by group 1 granitoids (Fig. 15). Collectively, these rocks, dominated by mafic and intermediate compositions, were derived by low-*P* partial melting of mafic crust containing the assemblage plagioclase + amphibole ± clinopyroxene ± garnet. Contemporaneous generation of less common granitoids having geochemical features indicative of high-*P* high-*T* partial melting of a clinopyroxene + garnet ± hornblende-bearing source, may reflect lower crustal anatexis at the base of a magmatically thickened proto-arc crust. The onset of apparently localized tectonism at ca. 2690–2685 Ma was accompanied by an increase in the volume of intermediate volcanic rocks and by the emplacement of voluminous intermediate plutonic rocks. These intermediate to felsic, volcanic and plutonic units have geochemical features indicative of dominantly high- and less commonly low-*P* partial melting of mafic sources. This is inferred to record the initiation of subduction beneath the proto-arc and the subsequent development of spaced, oceanic volcanic arc edifices.

The increase in the proportion of plutonic rocks having high-La signatures implies that shortly after ~2690 Ma, the magma source region became deeper, leaving garnet as a stable and abundant residual phase. This suggests that melting may have occurred within a subsiding or subducting slab. Alternatively, the change from extensional to compressional geodynamics at that time may have resulted in thickening of, and anatexis at, the base of the oceanic crust.

The latest magmatic activity in the belt included both the emplacement of rare potassic monzogranites inferred to have formed through high-*P* partial melting of thickened tonalitic crust, and the subsequent intrusion of rare, alkalic carbonatites, ijolites and syenites. These latter rocks are interpreted to represent very low-degree partial melts of metasomatically enriched lithospheric mantle, following termination of, or back-stepping of subduction.

Acknowledgements

Chris Hemmingway, Norah Brown, Thomas Hadlari and Yannick Beaudoin are thanked for assistance in the field. Reg Thériault and Klaus Sankowski assisted in the acquisition of the Nd isotopic data. The staff of the Geochemical Laboratories at the Geological Survey of Canada, Memorial University of Newfoundland and McGill University are thanked for the whole-rock analyses. We wish to thank A. Kerr and J. Tarney for insightful reviews of the paper. This is a contribution to the Western Churchill NATMAP project and is Geological Survey of Canada contribution #2003037 and Polar Continental Shelf Project contribution #01304.

Appendix A. Analytical methods

Approximately 1 kg of each rock sample was crushed to chips in a Braun jaw crusher, and a 50 g split of each was pulverized to a fine powder in either a tungsten carbide or an agate ring mill. Most analyses were obtained at the Geochemical Laboratories of the Geological Survey of Canada (GSC). Major elements and Ba were analyzed by X-ray fluorescence analysis (XRF) of fused discs. Volatile contents, expressed as loss on ignition (LOI) were determined gravimetrically. A further 114 specimens were selected for trace

and REE analysis. The trace elements Co, Cr, Cu, Ni, Sc, V and Zn were analysed by ICP-ES, whereas all other trace elements including Cs, Ga, Pb, Rb, Hf, Th, U, Ta, Nb, Y and the rare earth elements were determined through ICP-MS analysis on selected samples. Analytical errors for the data, as based on duplicate unknown analyses and analyses of reference materials are quoted at < 5% relative % for the major elements, <10% for those trace elements determined by XRF, <10% for ICP-ES analyses, <5% for ICP-MS analyses. These were supplemented by pressed powder disc, X-ray fluorescence analyses for the trace elements Rb, Sr, Y, Zr, Nb and Ga (Department of Earth and Planetary Sciences, McGill University).

Analysis of selected rock samples were undertaken at the Department of Earth Sciences, Memorial University of Newfoundland (MUN). Major elements and the trace elements were determined through XRF of glass discs. LOI was obtained gravimetrically. All other elements were obtained through ICP-MS analysis following the method of Longerich et al. (1990). Representative analyses of plutonic rocks of the region are presented in Table 2. Some analyses obtained at MUN lack LOI determinations.

Analytical procedures for Sm-Nd analyses are a variant of those documented by Thériault (1990). Whole-rock powders (ca. 0.2 g) were spiked with a ^{148}Nd–^{149}Sm mixed solution and dissolved in a warm HF-HNO_3 solution in teflon pressure capsules. Nd and Sm were separated using wet chemical chromatographic methods, ultra-pure acids and conventional cation specific separation resins. Isotopic ratios were determined by Thermal Ion Mass Spectrometry using a Finnigan Mat 261 solid source mass spectrometer run in the static mode. Neodymium isotopic compositions were normalized to $^{146}Nd/^{144}Nd = 0.7219$ and corrected to La Jolla $^{143}Nd/^{144}Nd = 0.511860$. Repeated analysis of an AMES standard Nd metal solution yielded $^{143}Nd/^{144}Nd = 0.512165 \pm 0.000020$ (2σ). Time corrected, Nd values were calculated using a present-day CHUR (chondritic uniform reservoir) composition of $^{143}Nd/^{144}Nd = 0.512638$ and $^{147}Sm/^{144}Nd = 0.1967$. The reproducibility of the ϵNd values, based on duplicate analyses, are ca. $\pm 0.5\epsilon$ units, whereas the reproducibility of the $^{147}Sm/^{144}Nd$ ratios is approximated at ca. 0.3%. Nd isotopic data for 14 samples along with 4 duplicate analyses are presented in Table 3.

References

Abbott, D., Drury, R., Smith, W.H.F., 1994. Flat to steep transition in subduction style. Geology 22, 937–940.

Arth, J.G., 1979. Some trace elements in trondhjemites-their implications to magma genesis and paleotectonic setting, In: Barker, F. (Ed.), Trondhjemites, Dacites, and Related Rocks. Elsevier, New York, pp. 123–132.

Arth, J.G., Barker, F., 1976. Rare-earth partitioning between hornblende and dacitic liquid and implications for the origin of trondjhemitic–tonalitic liquids. Geology 4, 534–536.

Ayer, J., Amelin, Y., Corfu, F., Kamo, S., Ketchum, J., Kwok, K., Trowell, N., 2002. Evolution of the southern Abitibi greenstone belt based on U–Pb geochronology: autochthonous volcanic construction followed by plutonism, regional deformation and sedimentation. Precambrian Res. 115, 63–95.

Barker, F. 1979. Trondhjemites: definition, environment and hypotheses of origin, In: Barker, F. (Ed.), Trondhjemites, Dacites and Related Rocks. Elsevier, Amsterdam, pp. 1–12.

Barker, F., Arth, J.G., 1976. Generation of trondhjemitic-tonalitic liquids and Archaean bimodal trondhjemite–basalt suites. Geology 4, 596–600.

Bédard, J.H., Brouillette, P., Madore, L., Berclaz, A., 2003. Archaean cratonization and deformation in the northern Superior Province, Canada: an evaluation of tectonic versus vertical tectonic models. Precambrian Res. 127, 61–87.

Bloomer, S.H., Taylor, B., MacLeod, C.J., Stern, R.J., Fryer, P., Hawkins, J.W., Johnson, L., 1995. Early arc volcanism and the ophiolite problem: a perspective from drilling in the western Pacific, In: Active Margins and Marginal Basins of the Western Pacific, Geophys. Monograph 88, Amer. Geophys. Union.

Cavell, P.A., Wijbrans, J.R., Baadsgaard, H., 1992. Archean magmatism in the Kaminak Lake area, District of Keewatin, Northwest Territories: ages of the carbonatite-bearing alkaline complex and some host granitoid rocks. Can. J. Earth Sci. 29, 896–908.

Choukroune, P., Ludden, J.N., Chardon, D., Calvert, A.J., Bouhallier, H., 1997. Archean crustal growth and tectonic processses: a comparison of the Superior Province, Canada and the Dharwar Craton, India. Geol. Soc. Spec. Pub. 121, 63–98.

Chown, E.H., Harrap, R., Moukhsil, A., 2002. The role of granitic intrusions in the evolution of the Abitibi belt, Canada. Precambrian Res. 115, 291–310.

Cousens, B.L., Aspler, L.B., Chiarenzelli, J.R. Geochemistry and Sm–Nd isotope composition of Neoarchean supracrustal and plutonic rocks, Henik segment, Central Hearne supracrustal belt, Nunavut, Canada. Precambrian Res., in press.

Davidson, A., 1968. An occurrence of alkali-syenite, Kaminak Lake map-area (55L) District of Keewatin. Geol. Surv. Can. Pap. 68 (1), 126–129.

Davidson, A., 1970a. Precambrian geology, Kaminak Lake map-area, District of Keewatin. Geol. Surv. Geol. Surv. Can. Pap. 69 (51), 27.

Davidson, A., 1970b. Kaminak Lake alkalic complex, District of Keewatin (55L). Geol Surv. Can. Pap. 70 (1A), 135–137.

Davis, W., Hanmer, S., Aspler, L., Sandeman, H., Tella, S., Zaleski, E., Relf, C., Ryan, J., Berman, R., MacLachlan, K.,

2000. Regional differences in the Neoarchean crustal evolution of the Western Churchill Province: can we make sense of it? GeoCanada 2000. Geological Association of Canada – Mineralogical Association of Canada Joint Annual Meeting, Calgary.

Davis, W.J., Hanmer, S., Sandeman, H.A, 2004. Temporal evolution of the Central Hearne supracrustal belt: rapid generation of juvenile crust in a suprasubduction zone setting. Precambrian Res. 134, 85–112.

Defant, M.J., Drummond, M.S., 1990. Derivation of some modern arc magmas by melting of young subducted lithosphere. Nature (London) 347, 662–665.

DePaolo, D.J., 1981. Neodymium isotopes in the Colorado Front Range and crust–mantle evolution in the Proterozoic. Nature 291, 193–196.

de Wit, M.J., Ashwal, L.D., 1997. Greenstone Belts. Clarendon Press, Oxford.

Drummond, M.S., Defant, M.J., 1990. A model for trondhjemite-tonalite-dacite genesis and crustal growth via slab melting: Archean to modern comparisons. J. Geophys. Res. 95, 21.

Drummond, M.S., Defant, M.J., Kepezhinskas, P.K., 1996. Petrogenesis of slab-derived trondhjemite-tonalite-dacite/adakite magmas. Trans. Royal Soc., Edinburgh 87, 205–215.

Hamilton, W.B., 1998. Archean magmatism and deformation were not products of plate tectonics. Precambrian Res. 91, 143–179.

Hanmer, S., Relf, C., 2000. Western Churchill NATMAP Project: new results and potential significance. GeoCanada 2000, Geological Association of Canada – Mineralogical Association of Canada Joint Annual Meeting, Calgary, CDROM format.

Hanmer, S., Peterson, T.D., Sandeman, H.A., Rainbird, R.H., Ryan, J.J., 1998. Geology of the Kaminak greenstone belt from Padlei to Quartzite Lake, Kivalliq Region, northwest territories, In: Current Research Geological Survey of Canada, Pap., 1998-C, pp. 85–94.

Hanmer, S., Sandeman, H.A., Davis, W.J., Aspler, L.B., Rainbird, R.H., Peterson, T.D., Ryan, J.J., Roest, W.R., Relf, C., Irwin, D. Tectonic setting of the Neoarchaean Henik–Kaminak–Tavani supracrustal belt, Western Churchill province, Canada: a geological perspective. Precambrian Res., in press.

Hanson, G.N., 1978. The application of trace elements to the petrogenesis of igneous rocks of granitic composition. Earth Plan. Sci. Lett. 38, 26–43.

Hoffman, P.F., 1988. United Plates of America, the birth of a craton: Early Proterozoic assembly and growth of Laurentia. Ann. Rev. Earth Plan. Sci. 16, 543–603.

Irvine, T.N., Barager, W.R.A., 1971. A guide to the chemical classification of the common volcanic rocks. Can. J. Earth Sci. 8, 523–548.

Irwin, D.A., Hanmer, S., Sandeman, H.A., Rainbird, R.H., Peterson, T.D., Relf, C., Ryan, J.J., Goff, S.P. Kerswill, J.A., 1998. Geology, Carr–Kaminak–Quartzite lakes area, Kivalliq region, Northwest Territories, Geological Survey of Canada, Open File Map 3649.

Irwin, D.A., 1994. Mineral occurences and preliminary geology of the Kaminak–Carr lakes area, District of Keewatin (parts of 55L/3, 4, 5 and 6). Northwest Territories Geol. Mapp. Div., Map EGS 1994-03, scale 1:50,000.

Jacobsen, S.B., Wasserburg, G.J., 1980. Sm–Nd isotopic evolution of chondrites. Earth Plan. Sci. Lett. 50, 139–155.

Kamber, B.S., Ewart, A., Collerson, K.D., Bruce, M.C., McDonald, G.D., 2002. Fluid-mobile trace element constraints on the role of slab melting and implications for Archaean crustal growth models. Contrib. Min. Petrol. 144, 38–56.

LeBas, M.J., LeMaitre, R.W., Streckeisen, A., Zanettin, B., 1986. A chemical classification of volcanic rocks based on the total alkali silica diagram. J. Petrol. 27, 745–750.

Le Maitre, R.W., 1989. A Classification of Igneous Rocks and Glossary of Terms. Blackwell, Oxford, UK.

Longerich, H.P., Jenner, G.A., Fryer, B.J., Jackson, S.E., 1990. Inductively coupled plasma – mass spectrometric analysis of geologic samples: a critical evaluation based on case studies. Chem. Geol. 83, 105–118.

Maniar, P.D., Piccoli, P.M., 1989. Tectonic discrimination of granitoids. Geol. Soc. Am. Bull. 101, 635–643.

Martin, H., 1986. Effect of steeper Archaean geothermal gradient on geochemistry of subduction-zone magmas. Geology 14, 753–756.

Martin, H., 1995. The Archean grey gneisses and the genesis of continental crust, In: Condie, K.C. (Ed.), Archean Crustal Evolution. Developments in Precambrian Geology 11. Elsevier, New York, pp. 205–258.

Martin, H., 1999. Adakitic magmas: modern analogues of Archaean granitoids. Lithos 46, 411–429.

Martin, H., Moyen, J., 2002. Secular changes in tonalite-trondhjemite-granodiorite composition as markers of the progressive cooling of Earth. Geology 30, 319–322.

Middelburg, J.J., Van der Weijden, C.H., Woittiez, J.R.W., 1988. Chemical processes affecting the mobility of major, minor and trace elements during weathering of granitic rocks. Chem. Geol. 68, 253–273.

Mueller, W.U., Marquis, R., Thurston, P.C., 2002. Evolution of the Archean Abitibi greenstone belt and adjacent terranes: new insights from geochronology, geochemistry, structure, and facies analysis. Precambrian Res. 115, 1–9.

Nisbet, E.G., Fowler, C.M.R., 1983. Model for Archean plate tectonics. Geology 11, 376–379.

Park, A.F., Ralser, S., 1992. Precambrian Geology of the Southwestern Part of the Tavani Map Area, District of Keewatin, Northwest Territories. Geolological Survey of Canada, Bulletin 416.

Pearce, J.A., 1982. Trace element characteristics of lavas from destructive plate boundaries, In: Thorpe R.S. (Ed.), Andesites. John Wiley and Sons, pp. 525–548.

Pearce, J.A., Cann, J.R., 1973. Tectonic setting of basic volcanic rocks determined using trace element analyses. Earth Plan. Sci. Lett. 19, 290–300.

Pearce, J.A., Harris, N.B.W., Tindle, A.G., 1984. Trace element discrimination diagrams for the tectonic interpretation of granitic rocks. J. Petrol. 25, 956–983.

Petford, N., Gallagher, K., 2001. Partial melting of mafic (amphibolitic) lower crust by periodic influx of basaltic magma. Earth Plan. Sci. Lett. 193, 483–499.

Rapp, R.P., Shimizu, N., Norman, M.D., Applegate, G.S., 1999. Reaction between slab-derived melts and peridotite in the mantle wedge: experimental constraints at 3.8 Gpa. Chem. Geol. 160, 335–356.

Relf, C. 1995. Geological map of the Snug Lake area, District of Keewatin (55L/8). Northwest Territories Geol. Mapp. Div., Map EGS 1995-00, scale 1:50,000.

Sandeman, H.A., Hanmer, S., Peterson, T.D., Davis, W.J., Ryan, J.J., 2004. Neoarchaean volcanic rocks, Central Hearne supracrustal belt, Western Churchill Province, Canada: geochemical and isotopic evidence supporting intraoceanic, suprasubduction zone extension. Precambrian Res. 134, 113–141.

Saunders, A.D., Tarney, J., 1991. Back-arc basins, In: Floyd P.A. (Ed.), Ocean Basalts. Blackie and Son, Glasgow, United Kingdom, pp. 219–263.

Scott, C.R., Mueller, W.U., Pilote, P., 2002. Physical volcanology, stratigraphy, and lithogeochemistry of an Archean volcanic arc: evolution from plume-related volcanism to arc rifting of SE Abitibi Greenstone belt, Val d'Or, Canada. Precambrian Res. 115, 223–260.

Sen, C., Dunn, T., 1994. Dehydration melting of basaltic composition amphibolite at 1.5 to 2.0 GPa: implications for the origin of adakites. Contrib. Min. Petrol. 117, 394–409.

Smithies, R.H., 2000. The Archaean tonalite-trondhjemite-granodiorite (TTG) series is not an analogue of Cenozoic adakite. Earth Plan. Sci. Lett. 182, 115–125.

Smithies, R.H., Champion, D.C., Cassidy, K.F., 2004. Formation of Earth's early Archaean continental crust. Precambrian Res. 127, 89–101.

Stern, R.J., Bloomer, S.H., 1992. Subduction zone infancy: examples from the Izu-Bonin-Mariana and Jurassic California arcs. Geol. Soc. Am. Bull. 104, 1621–1636.

Sun, S.S., McDonough, W.F., 1989. Chemical and isotopic systematics of oceanic basalts: implications for mantle composition and processes, In: Saunders, A.D., Norry, M.J. (Eds.), Magmatism in the Ocean Basins. Geolological Society Special Publication, vol. 42, pp. 313–345.

Taylor, S.R., McLennan, S.M., 1985. The Continental Crust: its Composition and Evolution. Blackwell Scientific Publications, Oxford.

Thériault, R.J., 1990. Methods for Rb–Sr and Sm–Nd isotopic analyses at the geochronology laboratory. Geol. Surv. Can. Geol. Surv. Can. Pap. 1989 (2), 3–6.

Thurston, P.C., Chivers, K.M., 1990. Secular variation in greenstone sequence development emphasizing Superior Province, Canada. Precambrian Res. 46, 21–58.

Tomlinson, K.Y., Condie, K.C., 2001. Archean mantle plumes: evidence from greenstone belt geochemistry. Geol. Soc. Am. Spec. Pap. 352, 341–357.

Villeneuve, M.E., Relf, C., 1998. Tectonic setting of 2.6 Ga carbonatites in the Slave Province, NW Canada. J. Petrol. 39, 1975–1986.

Whalen, J.B., 1985. Geochemistry of an island-arc plutonic suite: the Uasilau–Yau Yau intrusive complex, New Britain, P.N.G. J. Petrol. 26, 603–632.

Whalen, J.B., Syme, E.C., Stern, R.A., 1999. Geochemical and Nd isotopic evolution of Paleoproterozoic arc-type granitoid magmatism in the Flin Flon Belt, Trans-Hudson orogen, Canada. Can. J. Earth Sci. 36, 227–250.

Whalen, J.B., Percival, J.A., McNicoll, V.J., Longstaffe, F.J., 2002. A mainly crustal origin for tonalitic granitoids rocks, Superior Province, Canada: implications for late Archean tectonomagmatic processes. J. Petrol. 43, 1551–1570.

Wood, D.A., Joron, J.L., Treuil, M., 1979. A re-appraisal of the use of trace elements to classify and discriminate between magma series in different tectonic settings. Earth Plan. Sci. Lett. 45, 326–336.

Wright, G.M., 1967. Geology of the southeastern Barren Grounds, parts of the Districts of Mackenzie and Keewatin (Operations Keewatin, Baker, Thelon). Geol. Surv. Can. Memoir 350, 91.

Wyman, D.A., Kerrich, R., Polat, A., 2002. Assembly of Archean cratonic mantle lithosphere and crust: plume-arc interaction in the Abitibi-Wawa subduction–accretion complex. Precambrian Res. 115, 37–62.